Development 128, 1951-1969 (2001)
Printed in Great Britain © The Company of Biologists Limited 2001
DEV5903

A regulatory cascade of three homeobox genes, *ceh-10*, *ttx-3* and *ceh-23*, controls cell fate specification of a defined interneuron class in *C. elegans*

Zeynep Altun-Gultekin[1], Yoshiki Andachi[2], Ephraim L. Tsalik[1], David Pilgrim[3], Yuji Kohara[2] and Oliver Hobert[1,*]

[1]Department of Biochemistry and Molecular Biophysics, Center for Neurobiology and Behavior, Columbia University, College of Physicians and Surgeons, New York, NY 10032, USA
[2]Genome Biology Lab, Center for Genetic Resource Information, National Institute of Genetics, Mishima, Shizuoka, 411-8540, Japan
[3]Department of Biological Sciences, University of Alberta, Edmonton, Alberta T6G 2E9, Canada
*Author for correspondence (e-mail: or38@columbia.edu)

Accepted 27 February 2001

SUMMARY

The development of the nervous system requires the coordinated activity of a variety of regulatory factors that define the individual properties of specific neuronal subtypes. We report a regulatory cascade composed of three homeodomain proteins that act to define the properties of a specific interneuron class in the nematode *C. elegans*. We describe a set of differentiation markers characteristic for the AIY interneuron class and show that the *ceh-10* paired-type and *ttx-3* LIM-type homeobox genes function to regulate all known subtype-specific features of the AIY interneurons. In contrast, the acquisition of several pan-neuronal features is unaffected in *ceh-10* and *ttx-3* mutants, suggesting that the activity of these homeobox genes separates pan-neuronal from subtype-specific differentiation programs. The LIM homeobox gene *ttx-3* appears to play a central role in regulation of AIY differentiation. Not only are all AIY subtype characteristics lost in *ttx-3* mutants, but ectopic misexpression of *ttx-3* is also sufficient to induce AIY-like features in a restricted set of neurons. One of the targets of *ceh-10* and *ttx-3* is a novel type of homeobox gene, *ceh-23*. We show that *ceh-23* is not required for the initial adoption of AIY differentiation characteristics, but instead is required to maintain the expression of one defined AIY differentiation feature. Finally, we demonstrate that the regulatory relationship between *ceh-10*, *ttx-3* and *ceh-23* is only partially conserved in other neurons in the nervous system. Our findings illustrate the complexity of transcriptional regulation in the nervous system and provide an example for the intricate interdependence of transcription factor action.

Key words: Homeobox, *C. elegans*, Neuronal differentiation

INTRODUCTION

Differential gene expression patterns are a characteristic feature of individual cell types within the nervous system. Complex patterns of tightly controlled gene regulatory events are conferred by transcription factors that act at a variety of different stages during neuronal development. Some transcription factors act as early neuronal fate determinants such that their disruption leads to the adoption of distinct, non-neuronal cell fates. Other transcription factors function later in development to regionalize the nervous system, while the subsequent activity of yet other transcription factors determines specific subtype characteristics of neurons (Anderson and Jan, 1997; Bang and Goulding, 1996; Jurata et al., 2000). Transcription factors that act at distinct steps in the developmental history of a neuron most likely function in hierarchical cascades of gene regulation, in which early acting transcription factors turn on the expression of later acting transcription factors. The hierarchical activation of transcription factors presumably results in a progressive restriction in the developmental potential of a neuron, eventually leading to the acquisition of its terminal differentiation features. Transcriptional regulatory cascades have, for example, been described for neurogenic events involving bHLH proteins in vertebrates and flies (Anderson and Jan, 1997), cell fate determination in the vertebrate spinal cord (Edlund and Jessell, 1999; Tanabe et al., 1998), and cell subtype specification of a class of motoneurons (Baum et al., 1999) and touch sensory neurons (Mitani et al., 1993) in the nematode *C. elegans*.

A prominent class of transcription factors that acts to determine terminal differentiation characteristics of neurons is the LIM homeobox class of regulatory factors (Hobert and Westphal, 2000). In the mouse, *Isl1* is required for early aspects of motoneuron differentiation (Pfaff et al., 1996), while later acting Lhx genes, such as *Lhx3* or *Lhx4* define the identity of specific subtypes of motoneurons in the spinal cord (Sharma et al., 1998; Tsuchida et al., 1994). *Lim1* and *Lmx1b* coordinately direct axonal outgrowth

patterns in vertebrate limbs (Kania et al., 2000). In *Drosophila*, genetic and neuroanatomical studies on *apterous*, *islet* and *lim3* have revealed their involvement in several aspects of neuronal differentiation, including axon fasciculation, pathfinding and neurotransmitter choice (Lundgren et al., 1995; Thor et al., 1999; Thor and Thomas, 1997). As in vertebrates, combinatorial expression of Lhx genes in *Drosophila* determines motoneuron differentiation and axonal targeting choices in the ventral nerve cord (Thor et al., 1999).

As revealed by the genome sequencing project, *C. elegans* contains seven Lhx genes, which are expressed in largely non-overlapping sets of neurons (Hobert and Westphal, 2000). *mec-3*, one of the founding members of the Lhx gene family, represents the end-point in a cascade of transcriptional regulatory factors that determines the fate of touch sensory neurons (Mitani et al., 1993; Way and Chalfie, 1988). *mec-3* directly regulates the transcription of genes required for touch sensory neuron function such as the *mec-7* β-tubulin gene and the *mec-4* ion channel gene (Duggan et al., 1998). The *lin-11*, *lim-6* and *ceh-14* genes act to control as yet undefined subtype characteristics of specific neurons and other tissue types (Cassata et al., 2000; Freyd et al., 1990; Hobert et al., 1998; Hobert et al., 1999), while the *lim-4* gene functions as a binary cell-type switch in a class of odorsensory neurons (Sagasti et al., 1999).

There are three central aspects of Lhx gene function that remain poorly understood in any system. First, the precise nature of cellular defects evoked by loss of Lhx protein function is often unclear owing to the paucity of specific cell fate and neuroanatomical markers. Second, with a few exceptions (Benveniste et al., 1998; Duggan et al., 1998), target genes of Lhx proteins in the nervous system have remained largely elusive. Finally, the nature of upstream regulators of Lhx genes and hence the integration of Lhx gene function into larger transcriptional regulatory cascades or networks is little understood.

We address these key questions for the *C. elegans* Lhx gene *ttx-3*. We have previously shown that *ttx-3* mutant animals display defects in thermoregulatory behavior that mimic the defects seen upon ablation of a class of interneurons in the thermoregulatory neuronal circuit, the AIY interneuron class (Hobert et al., 1997). The expression of *ttx-3* in the AIY interneurons of wild-type animals hence suggested that *ttx-3* is required for the AIY neurons to function appropriately (Hobert et al., 1997). We now show that within the AIY interneurons *ttx-3* is part of a transcriptional regulatory cascade, which involves two other homeobox genes, *ceh-10* and *ceh-23*. We demonstrate that *ttx-3* is not required for the adoption of pan-neuronal features of the AIY interneurons but is rather required for the subtype specification of this interneuron class. We describe several genes that participate in defining AIY cell fate and that represent either direct or indirect targets of the *ttx-3* transcription factor. Neuroanatomical defects caused by loss of *ttx-3* function resemble those seen in axon pathfinding mutants, suggesting that *ttx-3* is also involved in determining patterns of axonal outgrowth. Furthermore, we show that a transcription factor regulated by *ttx-3*, the *ceh-23* homeobox gene, participates in the regulation of a presumptive *ttx-3* downstream target gene.

MATERIALS AND METHODS

Transgenic strains

Extrachromosomal arrays

adEx1450=Ex[ser-2::gfp; lin-15(+)] (courtesy of T. Niacaris and L. Avery)
otEx44 – otEx49, otEx97 – otEx101=Ex[ttx-3full::gfp; pRF4]
otEx57=Ex[ttx-3full::gfp; pBX]
otEx65=Ex[unc-119::ttx-3; pRF4]
otEx75=Ex[unc-33::gfp; unc-4(+)]
otEx93=Ex[pflp-1::gfp; pRF4]
otEx95, otEx96=Ex[unc-119::ttx-3; unc-122::gfp]; unc-122::gfp is a new injection marker (see below)
utEx54=Ex[C36B7.7::gfp; pRF4] (courtesy of T. Ishihara and I. Katsura).

Chromosomally integrated arrays

evIs111=integrated *Ex[F25B3.3::gfp;dpy-20(+)]* (kindly provided by Joe Culotti)
kyIs5IV=integrated *Ex[ceh-23::gfp; lin-15(+)]* (Forrester et al., 1998)
mgIs18IV and *mgIs32III*=independently integrated *Ex[ttx-3prom::gfp; plin-15]*
otIs7=integrated *Ex[zig-2::gfp; pRF4]* (O. Aurelio and O. H., unpublished)
otIs14=integrated *Ex[zig-3::gfp; pRF4]* (O. Aurelio and O. H., unpublished)
otIs24=integrated *Ex[sre-1::gfp; dpy-20(+)]*
otIs33IV=integrated *Ex[kal-1::gfp; pBX]* (H. Buelow and O. H., unpublished)
otIs45=integrated *Ex[unc-119::gfp]*
otIs62, otIs123=integrated *Ex[psra-11-3::gfp; pRF4]* and integrated *Ex[psra-11-3::gfp; unc-4(+)*], respectively
otIs97IV, otIs98, otIs99=integrated *otEx65*
otIs107=integrated *adEx1450*
otIs117=integrated *otEx75.*

The injection marker *pBX* was used in a *pha-1(e2123ts)* background; *unc-4(+)*, *lin-15(+)* and *dpy-20(+)* were used in *unc-4(e120)*, *lin-15(n765ts)* and *dpy-20(e1362)* backgrounds, respectively; and *pRF4* and *unc-122::gfp* in a wild-type background. (The protocol for integrating extrachromosomal arrays can be found at http://cpmcnet.columbia.edu/dept/gsas/biochem/labs/hobert/protocols.htm)

Behavioral assays

Thermotaxis assays were performed as described (Hedgecock and Russell, 1975). In our specific set-up, an aluminum slab bridged two water baths, one at 61°C, the other at 5°C; the ambient temperature was 25°C. Animals were grown at 20°C and assayed on a gridded 10 cm square petri dish that had equilibrated on the aluminum plate to establish a stable gradient from 22°C to 16.5°C (measured with a surface temperature probe). Animals were placed into the center of the gradient. After an assay time of 40-60 minutes, the animals were anaesthetized. For scoring, the plate was divided into six regions of 1.3 cm width (see Fig. 3A) and animals were counted in each region. Animals that had not left the 1.7 cm^2 quadrant in which they had been initially placed were not scored.

Dauer assays were performed by allowing four gravid adults per plate to lay eggs for 20 hours at 15°C. Adults were picked off and their offspring cultivated on an OP50 seeded plate at 25°C. After 3.5 days, the brood was scored. Animals that showed the characteristic thin elongated shape of dauers and displayed a characteristic dauer cuticle were scored as dauers; all the remaining animals at a stage older than L3 were scored as non-dauers. Many of the *daf-7; ttx-3* bypasser animals had transiently passed through a dauer-like, if not complete dauer stage, in which they remained for a variable amount of time. Hence, at the scoring time, dauer bypass mutants were

observed at all different stages (L3 to adults). The 'dauer bypass' phenotype thus encompasses a failure to enter the dauer stage, as well as a failure to appropriately arrest in the dauer stage.

Isolation and analysis of *ceh-23* null mutant animals

A *ceh-23* null allele was isolated using a transposon-tagging strategy (Zwaal et al., 1993). First, a Tc1 insertion in the *ceh-23* gene was isolated by PCR screening of a Tc1 library made from the MT3126 strain, using Tc1- and *ceh-23*-specific primers. The isolated strain YK16[*mut-2(r459); ceh-23(ms16::Tc1); dpy-19(n1347)III*] contained the Tc1 insertion in the last exon in the middle of the homeodomain at position 12957 (numbering of cosmid sequence ZK652). YK16 was then PCR screened for Tc1 excision events using *ceh-23*-specific primers. An imprecise Tc1 excision was identified in strain YK23[*mut-2(r459); ceh-23(ms23); dpy-19(n1347)III*] at position 11098-12961. The junction sequence is: 5′…TTGAGCTTT-G[deletion]AGTCGGAGCA…3′. YK23 was outcrossed several times with Bristol N2. As YK23 has no obvious phenotype, the genotype was scored using a triplex PCR, in which the three primers U2, D2 and D3 gave a 1 kb product on homozygous *ceh-23(ms23)* animals, a 1 kb/730 bp doublet on heterozygous animals and a 730 bp product on wild-type animals. The primer sequences are: U2, 5′-TACCTGCACAACACACTGAC-3′; D2, 5′-TGGCAAAATCATGG-CGGAAC-3′; and D3, 5′-TTGGATCCAGCAATTGTTTGAA-GAACGT-3′.

ceh-23::gfp expression in several neuron classes other than AIY, including ADF, ADL, AWC, AFD, PHA, PHB and CAN (Forrester et al., 1998), prompted us to assay differentiation of some of these neurons in *ceh-23* null mutants. We found that the AFD and ASE cell fate markers *gcy-8::gfp* and *gcy-5::gfp*, respectively, the ADF, ADL, PHA, PHB cell fate marker *srb-6::gfp*, the AWC cell fate marker *str-2::gfp* and the CAN cell fate marker *kal-1::gfp* were all correctly expressed in *ceh-23(ms23)* animals (data not shown). Moreover, ADL and PHA/PHB show normal dye filling behavior. In those cases where the neuron could be visualized in relative isolation (AFD, ASE, AWC, CAN, PHA/B), the anatomy of the neuron appeared wild type.

Genetic screen for new *ttx-3* alleles

To screen for new *ttx-3* alleles, we made use of two previously described consequences of loss of *ttx-3* function, the partial suppression of the dauer constitutive phenotype of a *daf-7* loss-of-function allele and the loss of positive autoregulation of the *ttx-3* gene (Hobert et al., 1997). A *daf-7(e1372)III; mgIs18IV* strain, that contains an integrated *ttx-3prom::gfp* array, was mutagenized with EMS at the L4 larval stage. The F_1 offspring were allowed to grow to the adult stage at 15°C. Eggs were prepared from these animals using standard bleaching protocols. Approximately 100-300 eggs of this F_2 generation were placed on single plates and cultivated at 25°C. Only plates that contained dauer bypass mutants quickly grew to starvation. Those plates were chunked and again grown to starvation at 25°C twice, in order to enrich for homozygous animals with the bypasser phenotype. Animals were isolated from plates that showed downregulated *ttx-3prom::gfp* expression, and after testing for X-linkage of the defect the *ttx-3* genomic locus was sequenced. Out of >100,000 haploid genomes screened, we retrieved three *ttx-3* alleles, *mg158*, *ot22* and *ot23*. In addition, we obtained another *ttx-3* allele, *nj14*, that was isolated by Ikue Mori in an independent screen for mutants that affect *ttx-3prom::gfp* expression.

Pan-neuronal marker genes

We reasoned that the *unc-33* gene, which appears to affect axon pathfinding throughout the nervous system (Hedgecock et al., 1985; McIntire et al., 1992), may be pan-neuronally expressed. We fused a 2.7kb genomic fragment that is immediately upstream to the start site of the previously described *unc-33 mRNA* transcript (Li et al., 1992) to *gfp* and found this reporter gene to be expressed throughout the whole nervous system (see Fig. 6A). Like *unc-119::gfp* (Maduro and Pilgrim, 1995), the *unc-33::gfp* reporter is expressed in dividing neuroblasts at pre-comma embryonic stages (data not shown). *unc-33::gfp* expression can be observed outside the nervous system in two amphid socket cells and weakly in non-neuronal pharyngeal cells. We also generated a fusion of the *gfp* gene to the promoter of the *F25B3.3* gene, the *C. elegans* ortholog of the Ca^{2+}-regulated *ras* nucleotide exchange factor CalDAG-GEFII/RasGRP, which is ubiquitously expressed in the vertebrate nervous system (Ebinu et al., 1998; Kawasaki et al., 1998). F25B3.3 and vertebrate CalDAG-GEFI/RasGRP both contain a unique combination of domains, a nucleotide exchange factor domain, two EF hands and a Cys-rich diacylglycerol binding motif; the respective *C. elegans* and rat proteins show 35% identity and 57% similarity throughout the whole length of the protein. The *F25B3.3::gfp* construct contains 3.5 kb genomic sequences upstream of the predicted ATG start site and the first six amino acids of the predicted protein and is exclusively expressed throughout the nervous system in *C. elegans* (see Fig. 6A). In contrast to *unc-119::gfp* and *unc-33::gfp*, which are already expressed in neuroblasts, *F25B3.3::gfp* is a postmitotic pan-neuronal marker, i.e. its onset of expression is observed after the terminal division of neurons (around 450 minutes of embryonic development; see Fig. 6B).

Pan-neuronal expression of *ttx-3*

The *unc-119::ttx-3* construct contains the genomic coding region of *ttx-3* from ATG to TGA cloned into the *unc-119* expression vector pBY103 (Maduro and Pilgrim, 1995). This construct was injected at 10 ng/μl together with either pRF4 (*rol-6*) or *unc-122::gfp* as injection marker into a *mgIs18; ttx-3(ks5)* strain to yield three independent transgenic lines, *otEx65*, *otEx95* and *otEx96*. All three lines show complete rescue of the autoregulatory defects of the *ttx-3(ks5)* mutation. *otEx65* was chromosomally integrated to yield three independent integrants, *otIs97*, *otIs98* and *otIs99*. All three extrachromosomal lines as well as all three integrated lines show ectopic *ttx-3prom::gfp* expression in RID and CAN (CAN expression is less consistent in *otEx95* and *otEx96*). *otEx95* and *otEx96* were assayed for thermotaxis behavior either in a wild-type or *ttx-3(ks5)* mutant background.

We examined ectopic expression of AIY fate markers other than *ttx-3prom::gfp* by using the extrachromosomal line *otEx65*, which we crossed with *otIs33* (*kal-1::gfp*), *kyIs5* (*ceh-23::gfp*), *otIs107 (ser-2::gfp)* and *otIs123 (sra-11::gfp)*. As *kal-1::gfp* and *ser-2::gfp* are already expressed in a substantial number of neurons in the head ganglia it was difficult to determine ectopic expression outside their normal expression domains in the head ganglia; it was clear, however, that pan-neuronal expression of *ttx-3* did not cause a significant broadening of the expression of either of the markers in the nervous system.

UNC-17 antibody staining

We used a modification of the freeze-cracking method kindly provided to us by J. Duerr. Briefly, mixed stage animals that were grown at 20°C were transferred onto poly-L-lysine coated slides and covered with a coverslip. Slides were then frozen in liquid nitrogen and animals were cracked by flipping coverslips off. Animals were quickly fixed in methanol and acetone, incubated in blocking serum and co-stained with mouse monoclonal anti-UNC-17 (kindly provided by J. Duerr and J. Rand) and polyclonal anti-GFP (Molecular Probes) antibodies.

Other DNA constructs

The *ttx-3* expression constructs *ttx-3resc* and *ttx-3prom::gfp* shown in Fig. 1B, have been described already (Hobert et al., 1997); *ttx-3full::gfp* represents a GFP PCR fusion product in which the genomic region contained within *ttx-3resc* has been PCR-fused to *gfp::unc-54-3′UTR* from the pPD95.75 vector. (Protocol for PCR fusion can be found at: http://cpmcnet.columbia.edu/dept/gsas/biochem/labs/hobert/protocols.htm). The *sra-11::gfp* construct is termed *psra-11-3::gfp* and contains

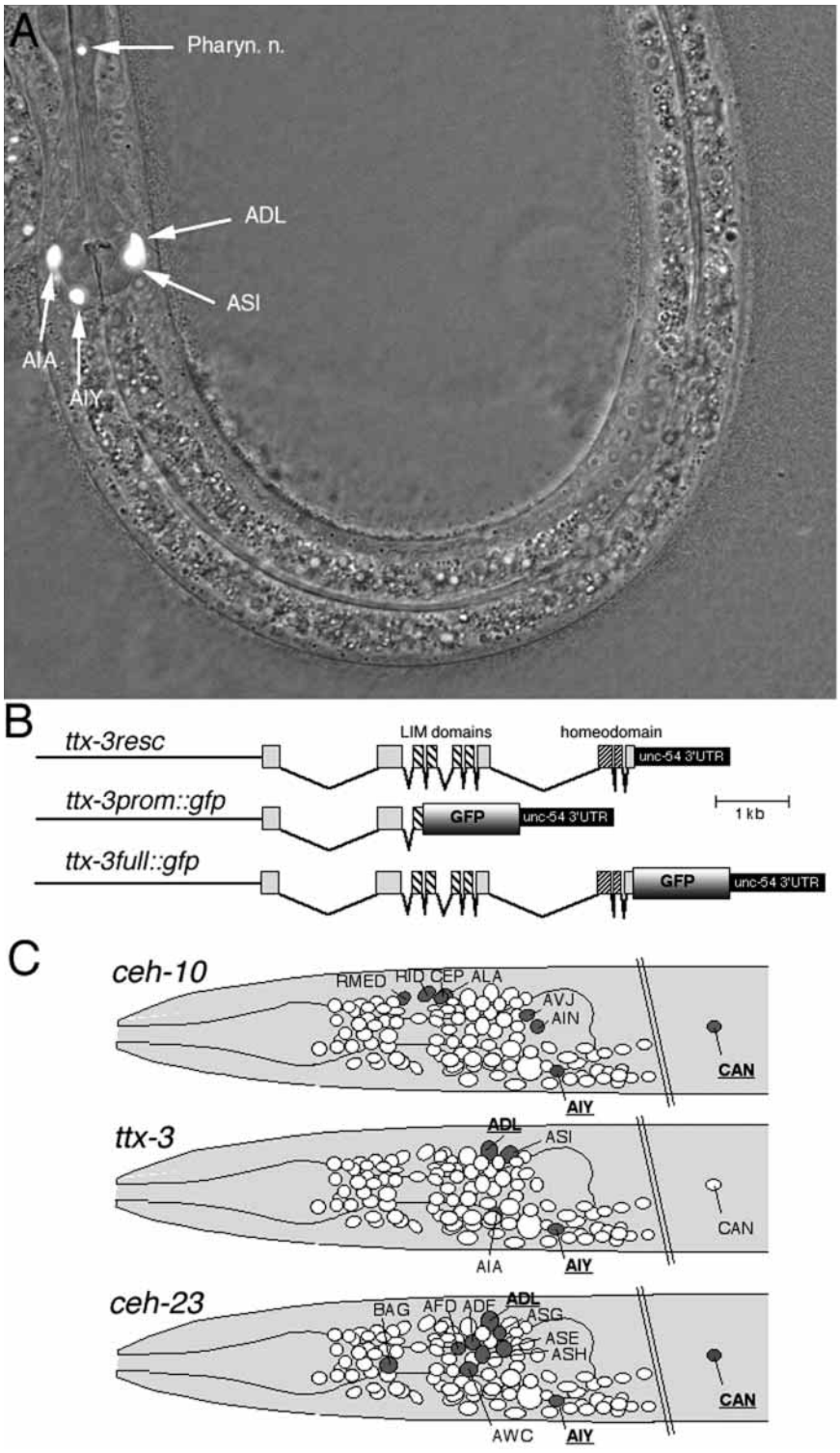

Fig. 1. Expression of homeobox genes in the AIY interneuron class. (A) Overlap of a DIC and a fluorescent image showing expression of a *ttx-3full::gfp* reporter gene construct (schematically shown in part B) in the nucleus of several head neurons of an early L2 stage animal. The fluorescent images were taken in several optical sections and layered upon each other. In this animal (genotype: *otEx57*) comparably strong expression can be seen in AIY, AIA, ADL and ASI. Within a population, 41/41 *otEx57* animals show strong expression in AIY and 39/41 show expression in AIA, 28/41 in ADL and 25/41 in ASI. Similar patterns of expression can be seen with a total of 12 independently obtained extrachromosomal arrays (*otEx45-otEx49, otEx57* and *otEx97-otEx101*). Pharyn. n., pharyngeal neuron. (B) Schematic representation of the expression constructs used. *ttx-3resc* rescues the thermotaxis phenotype of *ttx-3* mutant animals (Hobert et al., 1997), *ttx-3prom::gfp* reveals postembryonic expression exclusively in the AIY interneuron class (Hobert et al., 1997), *ttx-3full::gfp* expression is shown in A. (C) Schematic representation of the expression of *ceh-10::lacZ* (Svendsen and McGhee, 1995), *ttx-3full::gfp* (this study) and *ceh-23::gfp* (Forrester et al., 1998) reporter constructs in the *C. elegans* nervous system. Expression in neurons of the tail ganglia is not shown. The name of neurons in which expression of any of the three genes overlaps is bold and underlined.

a 3.9 kb *Xba*I genomic fragment, which encompasses most of the coding region of *sra-11* and 2.8 kb of sequence upstream of the predicted start codon. This construct is different from the one previously published (Troemel et al., 1995) and is more stably expressed in similar neuronal subtypes, namely AVB and AIY, but is also weakly expressed in AIA (see Fig. 5). The *flp-1::gfp* construct contains a genomic fragment from the 5′ region of the *flp-1* gene (Nelson et al., 1998), which extends from position –513 to –9 relative to the *flp-1* start codon. This construct is strongly and exclusively expressed in the AVK interneuron pair. *unc-122::gfp* is a reporter gene construct that is strongly and exclusively expressed in coloemocytes and used as an injection marker (P. Loria and O. H., unpublished). Genomic fragments were amplified by PCR and subcloned into the standard GFP vectors pPD95.75 or pPD95.77. *kal-1::gfp, zig-2::gfp, zig-3::gfp, ser-2::gfp* and *C36B7.7::gfp* will be described elsewhere.

RESULTS

Expression of three homeobox genes in the AIY interneurons

We have previously shown that a genomic fragment that contains 3.1 kb of sequence 5′ of the *ttx-3* translational start site as well as the first two exons and introns of the *ttx-3* gene directs expression of a *gfp* reporter gene to a single class of two bilaterally symmetric interneurons, AIYL and AIYR (Hobert et al., 1997). As additional regulatory elements for *ttx-3* gene expression may exist in more downstream located introns, we inserted *gfp* coding sequences into a genomic construct, which we had previously shown to rescue the *ttx-3* mutant phenotype; this construct contains 3.1 kb of 5′ upstream sequence and all exons and introns of the *ttx-3* gene (Fig. 1). Expression of this reporter gene construct is restricted to several head neurons throughout larval and adult stages (Fig. 1). The AIY interneuron class consistently expresses the reporter gene;

slightly weaker but still very consistent expression is also observed in the AIA interneuron class and less consistent and weaker expression can be observed in the ADL and ASI sensory classes as well as two pharyngeal neurons.

As shown schematically in Fig. 1C, two other homeobox genes are also expressed in AIY, *ceh-10* and *ceh-23*. *ceh-10* was identified by sequence homology to homeobox genes (Hawkins and McGhee, 1990) and independently in a screen for mutants affecting neuronal migration (Forrester et al., 1998); it contains a paired-type homeobox and represents the *C. elegans* ortholog of the vertebrate *Chx10/Chx10-1* genes, which are expressed in a restricted set of interneurons in the retina and spinal cord (Chen and Cepko, 2000). *ceh-23* was identified due to its proximity to the *C. elegans* Hox cluster (Wang et al., 1993) and represents a diverged homeobox gene with no clear ortholog in other species and no conserved motif outside the homeodomain (Fig. 2A).

Isolation of mutations in homeobox genes expressed in the AIY interneurons

We sought to define the regulatory relationship of *ceh-10*, *ttx-3* and *ceh-23* as well as their function in AIY interneuron differentiation by analyzing the loss-of-function phenotypes of these genes. To this end, we used the previously identified *ceh-10* null allele, *gm58* (Forrester et al., 1998) and newly identified *ttx-3* and *ceh-23* loss-of-function alleles, which we describe below.

ceh-23 mutant allele

We isolated a *ceh-23* deletion allele, *ms23*, through PCR-based screening of a Tc1 transposon library (see Materials and Methods). *ceh-23(ms23)* contains a 1864 bp deletion that extends from 301 bp 5′ of the ATG start codon into the last exon of the gene and deletes more than 75% of the coding sequence, including half of the homeobox (Fig. 2B). It is thus likely that this allele represents a complete loss-of-function allele. Despite expression of *ceh-23* in the CAN neurons, a neuron class that is essential for survival (Forrester and

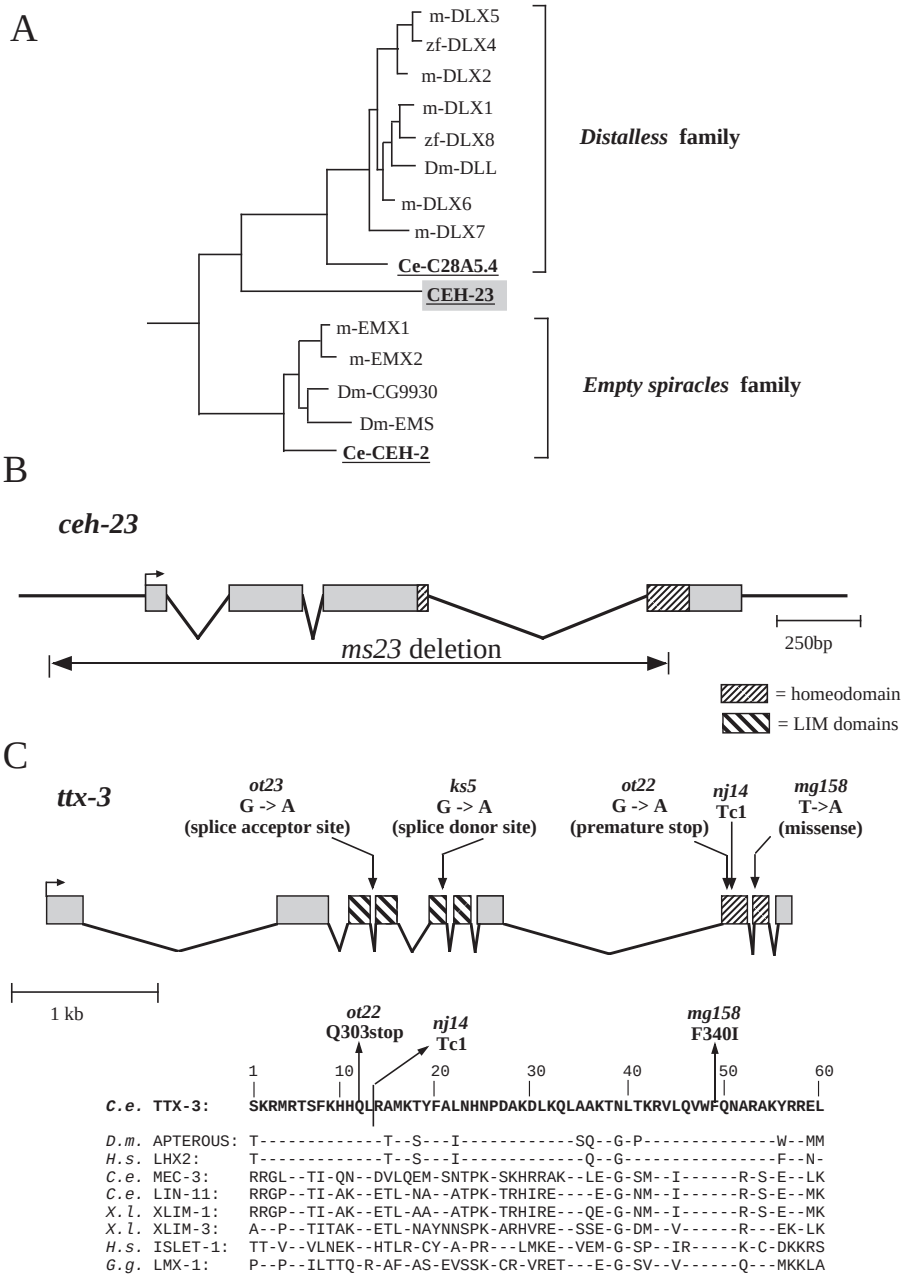

Fig. 2. *ceh-23* and *ttx-3* sequences and alleles. (A) Relationship of the CEH-23 homeodomain to its most closely related homeodomains. Although the CEH-23 homeodomain bears a strong affinity to the *distal-less* and *empty spiracles* protein families, other *C. elegans* proteins represent the true *Dll* and *ems* orthologs. CEH-23 appears to have no ortholog in other species, suggesting that CEH-23 may have arisen by a gene duplication event in the nematode lineage. *C. elegans* proteins are bold and underlined. Homeodomains that show the highest similarity to the CEH-23 homeodomain were identified by BLAST searches (including searches of the 11/23/00 release of the *C. elegans* genome, the 11/6/2000 release of the human genome sequence and the 9/16/2000 release of the *Drosophila* genome sequence) and assembled into a phylogenetic tree using the pileup/distances/growtree algorithms of the GCG package with default parameters. The tree is rooted with LIM and POU homeodomain proteins (not shown). (B) *ceh-23(ms23)* deletion allele. (C) *ttx-3* mutant alleles. The upper panel shows the schematic localization of the nucleotide changes in *ttx-3* alleles. The lower panel shows the corresponding amino acid changes in the homeodomain. *mg158* contains a missense mutation in one of the most highly conserved residues of the homeodomain, F49 (homeodomain numbering), which appears to be indispensable for the structural integrity of homeodomains (Gehring et al., 1994). *nj14* was provided by Ikue Mori; due to its molecular similarity to *ot22*, it was not further characterized.

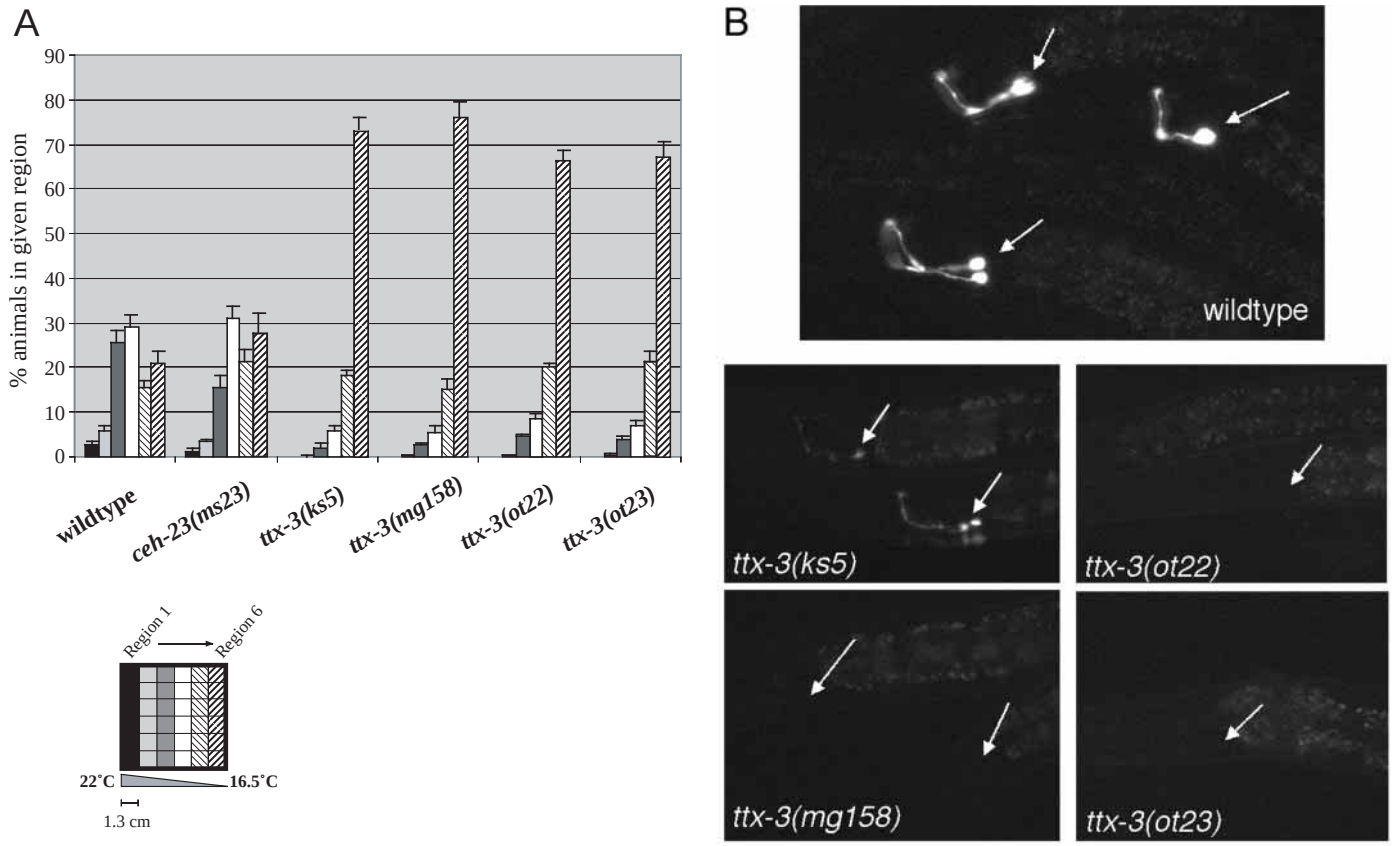

C

ttx-3prom::gfp expression in AIY	*wildtype*	*ttx-3(ks5)*	*ttx-3(ot22)*	*ttx-3(ot23)*	*ttx-3(mg158)*
strong	99%	10%	0%	0%	0%
dim	1%	75%	4%	2%	8%
very dim	0%	0%	23%	5%	2%
undetectable	0%	15%	73%	93%	90%
n	94	129	81	71	66

D

genotype	bypasser at 25˚C	*n*
daf-7(e1372)	1%	489
daf-7(e1372); ttx-3(ks5)	45%	558
daf-7(e1372); ttx-3(ot22)	63%	493
daf-7(e1372); ttx-3(ot23)	53%	256
daf-7(e1372); ttx-3(mg158)	62%	635
daf-7(e1372); ceh-23(ms23)	1%	650

Fig. 3. Phenotypic characterization of *ttx-3* and *ceh-23* alleles. (A) Thermotaxis assays (see Materials and Methods). Animals were grown at 20°C. Number of assays per genotype: wild type N2=11; *ceh-23(ms23)*=8; *ttx-3(ks5)*=6; *ttx-3(mg158)*=6; *ttx-3(ot22)*=7; *ttx-3(ot23)*=8. For each genotype, an average of 284-417 animals were tested per assay. The error bars represent the standard error of the mean. The difference in cryophilic behavior between wild type and *ceh-23(ms23)* is not statistically significantly different ($P>0.3$; paired and unpaired Student's *t*-test). Our observation of a certain fraction of wild-type animals showing cryophilic behavior is consistent with previous reports (Hedgecock and Russell, 1975; Mori and Ohshima, 1995). (B) Effect of *ttx-3* alleles on the level of *ttx-3prom::gfp* expression in AIY (white arrows point to AIYL/R in different animals). All animals shown contain the integrated *ttx-3prom::gfp* array *mgIs18*, which was crossed into the respective mutant backgrounds. In *ks5* mutant animals signal strength of *mgIs18* is clearly reduced, yet enough freely diffusible GFP protein is made in the cell to allow visualization of the axons. In contrast, *mgIs18* expression is mostly undetectable in *mg158*, *ot22*, and *ot23* mutants. (C) Quantification of the defects shown in B. 'Dim' refers to clearly reduced *gfp* expression with the axons being barely visible, 'very dim' to *gfp* expression that is insufficient to visualize the axons. (D) Dauer assays (see Materials and Methods). Results are from four experiments.

Garriga, 1997), *ceh-23(ms23)* mutant animals are viable and display no obvious neuroanatomical, morphological or locomotory abnormalities (see Materials and Methods).

ttx-3 mutant alleles

Prior to this study, only one *ttx-3* allele, *ks5*, was available. *ks5* mutant animals show thermotaxis defects that are similar to those seen in animals in which the AIY interneurons have been ablated; additionally, when placed over a chromosomal deficiency, *ttx-3(ks5)* behaves as a complete loss-of-function allele (Hobert et al., 1997). However, the molecular nature of *ks5*, a splice site mutation, left open the possibility that small amounts of truncated and partially active TTX-3 protein could be generated through incorrect splicing. To undertake a detailed analysis of AIY interneuron fate in *ttx-3* mutants, we thus sought to identify new mutant alleles of the *ttx-3* gene, whose molecular nature may more unambiguously imply a complete loss of *ttx-3* function. Through screening for mutants with characteristic *ttx-3*-like defects, we identified a total of three new *ttx-3* alleles, termed *mg158*, *ot22* and *ot23* (see Materials and Methods). All three alleles result in characteristic thermotaxis defects (Fig. 3A), which mimic the thermotaxis defects seen upon laser ablation of the AIY interneurons (Mori and Ohshima, 1995). Each allele was

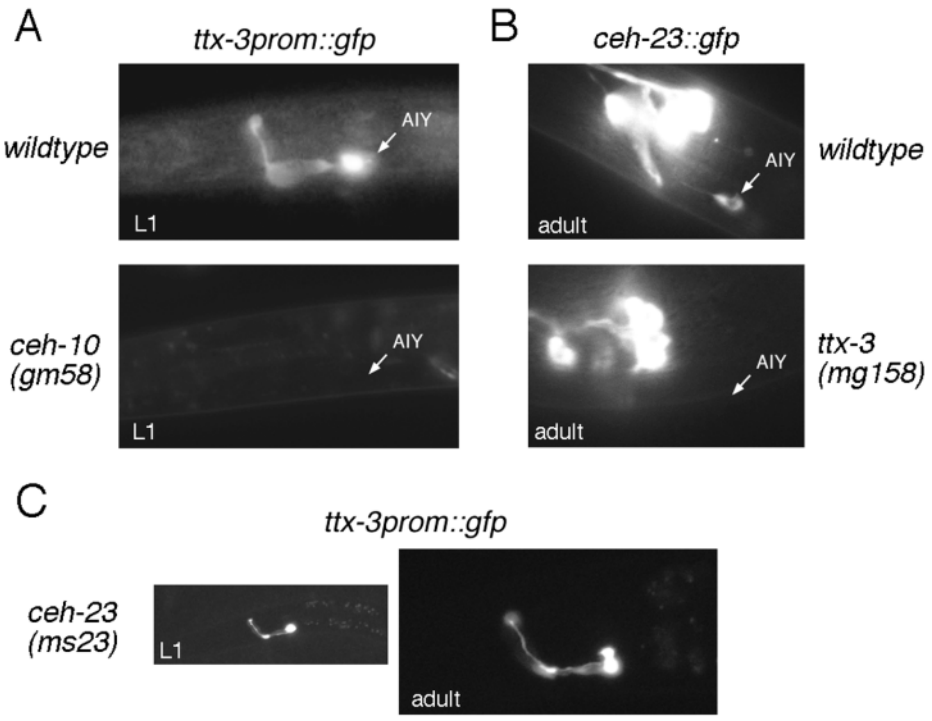

Fig. 4. Regulation of homeobox gene expression in AIY. (A) *ttx-3prom::gfp* expression is absent in *ceh-10(gm58)* animals. Homozygous *ceh-10(gm58*) offspring of *ceh-10(gm58)/+; mgIs18* hermaphrodites arrest as L1 larvae and were identified based on their *clr* phenotype. Expression was never observed (*n*>50). (B) *ceh-23::gfp* expression is dependent on *ttx-3*. Adult *ttx-3(mg158); kyIs5* were scored. Quantification is shown in Table 1. (C) *ttx-3prom::gfp* expression is unaffected in *ceh-23(ms23)* null mutant animals (*n*>50). Note the morphological integrity of the AIY neuron in terms of its cell position and axon morphology.

Table 1. Expression of AIY subtype markers in *ttx-3* and *ceh-23* mutant animals

		Wild type‡		*ttx-3 (ks5)*§		*ttx-3 (mg158)*§		*ceh-23 (ms23)*§	
AIY cell fate marker*		L1	Adult	L1	Adult	L1	Adult	L1	Adult
ttx-3	Homeobox	100 (*n*=94)	99 (*n*=104)	7 (*n*=128)	10 (*n*=129)	0 (*n*=45)	0 (*n*=72)	100 (*n*=56)	100 (*n*=79)
ceh-23	Homeobox	87 (*n*=55)	100 (*n*=67)	8 (*n*=40)	0 (*n*=117)	11 (*n*=47)	0 (*n*=87)	N.D.	N.D.
sra-11	Orphan 7TMR	92 (*n*=73)	75 (*n*=49)	0¶ (*n*=75)	4¶ (*n*=89)	0 (*n*=84)	0 (55)	94 (53)	4 (105)
ser-2	Putative metabotropic 5-HT receptor	84 (*n*=32)	91 (*n*=24)	19 (*n*=21)	30 (*n*=91)	27 (*n*=26)	26 (*n*=83)	83 (*n*=24)	85 (*n*=80)
kal-1	Secreted protein	95 (*n*=21)	92 (*n*=92)	6 (*n*=29)	0 (*n*=97)	2 (*n*=37)	2 (59)	94 (*n*=32)	93 (*n*=56)
C36B7.7	Secreted protein	70 (*n*=36)	83 (*n*=143)	44 (*n*=54)	35 (*n*=59)	41 (*n*=43)	38 (*n*=26)	65 (*n*=20)	79 (*n*=73)
unc-17	Vesicular acetylcholine transporter	N.D.	87 (*n*=46)	N.D.	26 (*n*=24)	N.D.	N.D.	N.D.	93 (*n*=70)

As residual expression of some AIY differentiation markers is still occasionally observed in the absence of *ttx-3* function, we tested whether *ceh-23* has a supplementary but non-essential role in *ttx-3* dependent gene regulatory events. For example, a residual amount of CEH-23 protein may still be expressed in *ttx-3* mutants and be able to induce small amounts of expression of *ttx-3*-dependent target genes. We tested this possibility by examining AIY marker gene expression in *ceh-23; ttx-3* double mutants and found that the defects were no worse than in the *ttx-3* single mutant (data not shown). Thus, while *ttx-3* and *ceh-23* apparently both contribute to the regulation of the *sra-11* gene, the regulation of other *ttx-3* target genes appears to be entirely independent of *ceh-23* function.

*Cell fate marker expression was monitored by antibody staining (*unc-17*) or by examining the expression of *gfp* reporter gene constructs (*ttx-3*: *mgIs18, ceh-23: kyIs5, sra-11: otIs62, ser-2: adEx1450, kal-1: otIs33, C36B7.7: utEx54*) that were crossed into the respective mutant backgrounds. Expression of the reporter gene in wild-type and mutant phenotypes were compared side-by-side.

‡Numbers are percentages of animals that show expression of the respective marker in the AIY interneuron class.

§Numbers are percentages of mutant animals that show 'wild-type-like' expression levels of the respective marker. 'Non-wild-type-like' expression can be subdivided into weak but detectable expression or entirely absent expression.

¶We had previously noted effects of *ttx-3(ks5)* on *sra-11::gfp* expression from an extrachromosomal array, yet found a substantial number of *ttx-3(ks5)* animals that still express the reporter (Fig. 5B in Hobert et al., 1997). Here, we use a distinct *sra-11::gfp* construct (see Materials and Methods) that is expressed from a chromosomally integrated array.

N.D., not determined.

defective in autoregulation of a *ttx-3prom::gfp* reporter gene (Fig. 3B,C) and suppressed the dauer-constitutive phenotype of *daf-7(e1372)* at 25°C (Fig. 3D). While the behavioral defects of the new alleles were comparable with those seen in the previously available *ks5* allele, the autoregulatory defects of the new alleles were stronger than in those observed with the *ks5* allele (Fig. 3B,C). Sequencing of the new *ttx-3* alleles confirmed the notion that at least two of them (*mg158, ot22*) are likely to be null for *ttx-3* function (Fig. 2C).

ceh-10, ttx-3 and *ceh-23* constitute a regulatory cascade of transcription factors in the AIY neurons

The availability of mutant alleles in all three homeobox genes has allowed us to address whether these transcriptional regulators act either in a linear pathway or, alternatively, in independent pathways within the AIY interneuron class. In a presumptive linear pathway, *ceh-10* would likely be the most upstream acting gene, as *ceh-10* expression in AIY is only observed during embryogenesis and fades after hatching

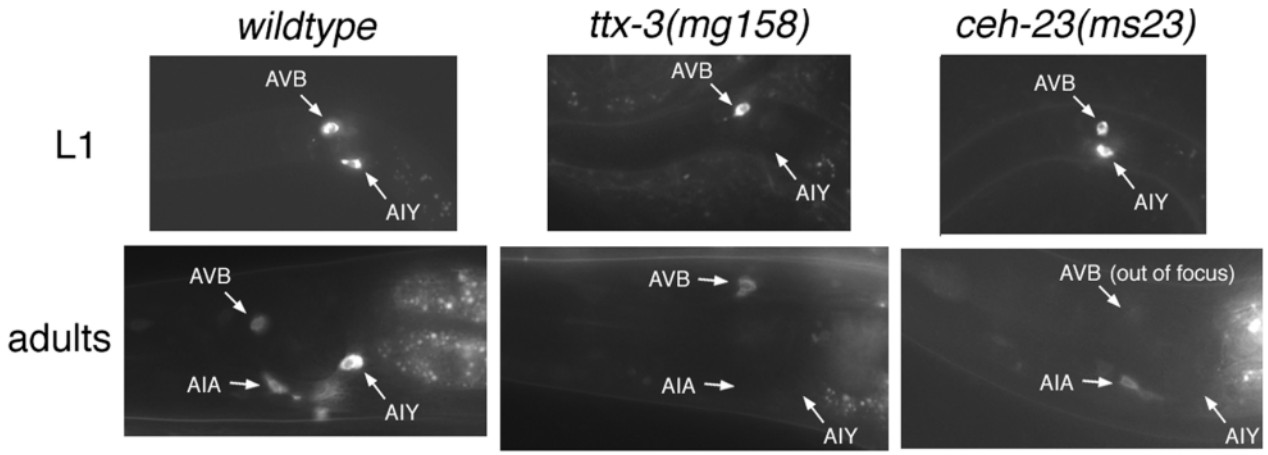

Fig. 5. Expression of the AIY cell fate marker *sra-11::gfp* in *ttx-3* and *ceh-23* mutant animals. *sra-11::gfp* expression was monitored by mating *otIs62* animals that harbor an integrated *sra-11::gfp* construct with animals of the respective mutant backgrounds. The animals carry a *rol-6* injection marker, leading to a slight distortion in the spatial arrangement of neurons. Quantification of the expression data in the AIY interneurons is shown in Table 1. While expression of *sra-11::gfp* in AVB is strong and highly penetrant in L1 larvae, it is observed less consistently and more weakly in adult animals (compare upper and lower panels; this observation was made with three independently created integrants, *otIs62*, *otIs122* and *otIs123*). Expression of *sra-11::gfp* in AVB came to lie out of the plane of focus in the *ceh-23(ms23); otIs62* adult animal shown in the lower right panel. Expression of *sra-11::gfp* in AIA is difficult to consistently detect in larvae, yet clearly visible in adult animals. 64% of wild-type adults show expression (n=45) in AIA and 38% (n=70) of *ttx-3(mg158); otIs62* adults show expression in AIA (see lower middle panel).

(Svendsen and McGhee, 1995), while expression of both *ttx-3* and *ceh-23* is initiated in embryogenesis and maintained throughout adulthood (data not shown). Thus, we first tested whether *ceh-10* is involved in initiation of *ttx-3prom::gfp* and *ceh-23::gfp* expression. We found that in the *ceh-10* null allele *gm58, ttx-3prom::gfp* expression is abolished in the AIY interneurons (Fig. 4A). Conversely, a *ceh-10::lacZ* reporter gene construct is still expressed in *ttx-3* mutants (data not shown). Forrester et al. have previously shown that *ceh-10* is required for *ceh-23::gfp* expression in AIY (Forrester et al., 1998). These findings demonstrate that *ceh-10* either directly or indirectly regulates both *ttx-3* and *ceh-23* expression.

To elucidate the regulatory relationship between *ttx-3* and *ceh-23*, we examined *ceh-23::gfp* expression in *ttx-3* mutant animals and found that loss of *ttx-3* function leads to an almost complete loss of *ceh-23::gfp* expression in AIY (Fig. 4B; Table 1). Conversely, *ttx-3prom::gfp* expression was unaffected in *ceh-23* null mutants (Fig. 4C; Table 1). Thus, *ceh-10, ttx-3* and *ceh-23* act in a linear regulatory cascade in the AIY interneurons with *ceh-10* regulating the expression of *ttx-3*, which then controls *ceh-23* expression.

AIY differentiation can be monitored by expression of a series of cell fate markers

We next investigated how the *ceh-10→ttx-3→ceh-23* regulatory cascade couples to AIY interneuron development and function. Cell type diversification in the nervous system is a consequence of differential gene expression within a given neuronal subtype. Hence, individual neuronal subtypes are defined by the expression of a specific and unique combination of molecular markers. The AIY interneuron class can be described by such a unique combinatorial gene expression profile: in a genome-sequence based survey of expression patterns of putative neuronal cell surface molecules, we identified a FnIII-domain-containing cell surface protein with homology to the human Kallmann's syndrome gene, termed KAL-1, which is expressed in AIY and several other head neurons (H. Buelow, Z. A.-G. and O. H., unpublished). As the AIY neurons may constitute an integration point of temperature and food sensory inputs (Hobert et al., 1997; Mori and Ohshima, 1995) and since serotonin (5-HT) is involved in food signaling (Sze et al., 2000), we reasoned that 5-HT receptors may be expressed in AIY; we indeed found that a seven-transmembrane receptor with similarity to 5-HT and octopamine receptors, termed SER-2 (identified by T. Niacaris and L. Avery), is expressed in AIY. Moreover, an orphan serpentine receptor of unknown function, SRA-11 (Troemel et al., 1995), an acetylcholine transporter protein, UNC-17 (Alfonso et al., 1993; J. Duerr and J. Rand, personal communication) and a novel secreted protein of unknown function, C36B7.7 (T. Ishihara and I. Katsura, pers.comm.) had been previously identified as being expressed in AIY and several other neurons. While the expression of none of these eight markers (*ceh-10*, *ttx-3*, *ceh-23*, *kal-1*, *ser-2*, *sra-11*, *unc-17* and *C36B7.7*) is entirely restricted to AIY, the expression of all eight markers exclusively overlaps in the AIY interneuron class. AIY thus has a unique 'address', which defines its identity and allows it to be distinguished from other neurons. This 'address' has enabled us to investigate if and how the three homeobox genes *ceh-10, ttx-3* and *ceh-23* influence AIY interneuron differentiation.

ceh-23 is required to maintain one feature of the AIY differentiation program

We examined the function of *ceh-23*, the transcription factor that is most downstream in the *ceh-10→ttx-3→ceh-23* cascade, by analyzing the expression of AIY marker genes in a *ceh-23* null mutant background. We found that *ceh-23* has no impact on the regulation of *kal-1, C36B7.7, ser-2* and *unc-17* expression, yet it affects expression of the orphan seven transmembrane receptor *sra-11*. While *sra-11::gfp* expression in *ceh-23(ms23)* L1 larvae appears normal, expression decreases significantly in adult animals (Fig. 5 and Table 1).

We also tested whether *ceh-23* is required for the known functions of the AIY interneurons, thermotaxis and dauer arrest. Both behaviors were normal in *ceh-23(ms23)* mutant animals (Fig. 3A,D). We also observed that AIY interneuron structure, i.e. cell body position and axon morphology appears wild-type in *ceh-23* null mutants (Fig. 4C). In summary, *ceh-23* has no role in the regulation of known aspects of AIY function, but it is required for the maintenance of one AIY differentiation characteristic, the expression of the *sra-11* gene. Additionally, *ceh-23* may affect other as yet unknown parameters of AIY structure and function.

ttx-3 is required for the expression of all known subtype-specific aspects of AIY interneuron differentiation

The finding that loss of *ceh-23* function has neither an obvious effect on axonal morphology of the AIY interneurons nor on the known behaviors mediated by the AIY interneurons demonstrates that the function of *ttx-3*, the upstream regulator of *ceh-23*, must go beyond regulation of the *ceh-23* gene, as *ttx-3* animals display severe axonal and functional defects of the AIY interneurons (Fig. 3 and see Fig. 7). We examined parameters of AIY differentiation in *ttx-3(mg158)* mutant animals using the AIY cell fate markers described above. We found that the expression of every known AIY subtype marker depends on *ttx-3* function (Fig. 5 and Table 1). Expression of *ceh-23, kal-1, C36B7.7, ser-2, unc-17* and *sra-11* is either significantly reduced or absent in *ttx-3(mg158)* and *ttx-3(ks5)* mutant animals (Fig. 5 and Table 1). As shown in Fig. 5, the effect of loss of *ttx-3* function on expression of the *sra-11* gene is stronger (loss in larvae and adults) when compared with the loss of *ceh-23* function (loss only in adults), suggesting that the effect of *ttx-3* on *sra-11* gene expression cannot be solely explained by loss of *ceh-23* function. Rather, both *ttx-3* and *ceh-23* seem to be contributing individually to the regulation of *sra-11* expression. The finding that *ttx-3* is required for expression of all known AIY subtype markers is in accordance with the complete loss of AIY function in thermotaxis and dauer arrest as shown in Fig. 3 and suggests that *ttx-3* is a central regulator of AIY interneuron differentiation. At this point it can not be assessed how aberrant expression of these marker genes relates to the defects of AIY structure and function in *ttx-3* mutants, as mutations in these marker genes have – with the exception of *unc-17* – not been described so far. *unc-17* null mutants die as embryos (Alfonso et al., 1993) and can thus not be readily tested for AIY structure and function. *unc-17* hypomorphs show normal AIY morphology (see Table 3).

As loss of *ttx-3* function causes the AIY interneurons to adopt a variably defective axon morphology which is unlike that of any other neuron, we consider it unlikely that a complete transformation from AIY fate to the fate of another neuron has taken place. We nevertheless tested this possibility by examining the expression of a spectrum of markers for other cell fates in *ttx-3* mutant animals. We monitored fate markers expressed in cells that are related to AIY by either lineage, synaptic connectivity, function or axon morphology (Table 2). We found that none of these markers are ectopically activated in AIY in *ttx-3(mg158)* mutant animals and thus found no evidence that AIY has adopted other distinct cell fate features (Table 2). We instead favor the possibility that AIY has simply lost several, if not all, of its subtype-specific characteristics and remains in an at least partially undifferentiated state.

Table 2. Neuronal cell fate analysis in *ttx-3* mutant animals

Neuronal cell type		Cell fate marker*	Expression in *ttx-3(mg158)*	
			In wild-type location‡	Ectopically in AIY
Cells that are related to AIY by lineage§	SMDD	*ZC21.2::gfp*	+	–
	AVK	*flp-1::gfp*	+	–
	AWC	*str-2::gfp*	+	–
	AVL	*unc-25::gfp*	+	–
Cells that are synaptically connected to AIY and/or functionally related¶	AIZ	*lin-11::gfp*	+	–
	AFD	*gcy-8::gfp*	+	–
	AWA	*odr-10::gfp*	+	–
	ASE	*gcy-5::gfp*	+	–
	AWC	*str-2::gfp*	+	–
Cells with AIY-like axon projections and/or similar cell body position**	AIM	*zig-3::gfp*	+	–
	AVK	*flp-1::gfp*	+	–
Cells that express *ttx-3* in wild-type animals	ADL	*srb-6::gfp*	+	–
	ADL	*sre-1::gfp*	+	–
	ASI	*srd-1::gfp*	+	–
	ASI	*osm-10::gfp*	+	–
	ASI	*daf-7::gfp*	+	–
	ASI	*zig-2::gfp*	+	–
	ASI	*zig-3::gfp*	+	–
	AIA	*sra-11::gfp*	+/–‡‡	–

**ZC21.2::gfp=kyIs123* (Colbert et al., 1997); *flp-1::gfp=otEx93* (Materials and Methods); *str-2::gfp=kyIs140* (Sagasti et al., 1999); *unc-25::gfp=juIs8* (Jin et al., 1999); *lin-11::gfp=mgIs21* (Hobert et al., 1998); *gcy-5::gfp=ntIs1; gcy-8=oyIs17* (Yu et al., 1997); *odr-10::gfp=kyIs37* (Sengupta et al., 1996); *zig-2::gfp=otIs7, zig-3::gfp=otIs14* (O. Aurelio and O. H., unpublished); *srb-6::gfp=gmIs12; sra-11::gfp=otIs62* (Troemel et al., 1997); *daf-7::gfp=saIs7* (Schackwitz et al., 1996). Reporter gene arrays were crossed into *ttx-3(mg158)* animals.

‡+, animals that show expression that is comparable with wild-type expression (n>20).

§This category includes neurons that show a lineage history that differs from AIYL/R at only one step in the invariant cell division pattern that generates AIYL/R (Sulston, 1983).

AIYL/R:	AB	`pl/rpapaaap`	
SMDDL/R:	AB	`--/-------a`	(=sister cell)
AVKL/R:	AB	`--/-----p--`	
AVL:	AB	`--/-----p--`	
AWCL/R:	AB	`--/---a----`	

¶AIY receives major synaptic input from the AFD, AWA, AWC and ASE sensory neurons and makes prominent synapses onto AIZ (White et al., 1986). AFD, AIY and AIZ are functionally interconnected neurons in the thermotaxis circuit (Mori and Ohshima, 1995).

**AIML, AIYL and AVKL are located in a characteristic row of three cells behind the excretory cell in adult animals (Sulston et al., 1983; White et al., 1986). Additionally, AIM extends a monopolar axon into the nerve ring that closely resembles that of AIY (White et al., 1986).

‡‡ *sra-11::gfp* expression of the *otIs62* strain in the AIA interneurons is observed in 64% of wild-type animals (n=45) and 38% (n=70) of *ttx-3(mg158); otIs62* animals.

ttx-3 and *ceh-10* separate pan-neuronal from subtype-specific characteristics

In *ttx-3* mutant animals, the AIY interneuron class may have either completely lost all components of its neuronal identity or it may have exclusively lost subtype-specific aspects of its differentiation program, while still maintaining nonspecific aspects of neuronal identity. We set out to distinguish between these possibilities by examining the expression of reporter gene

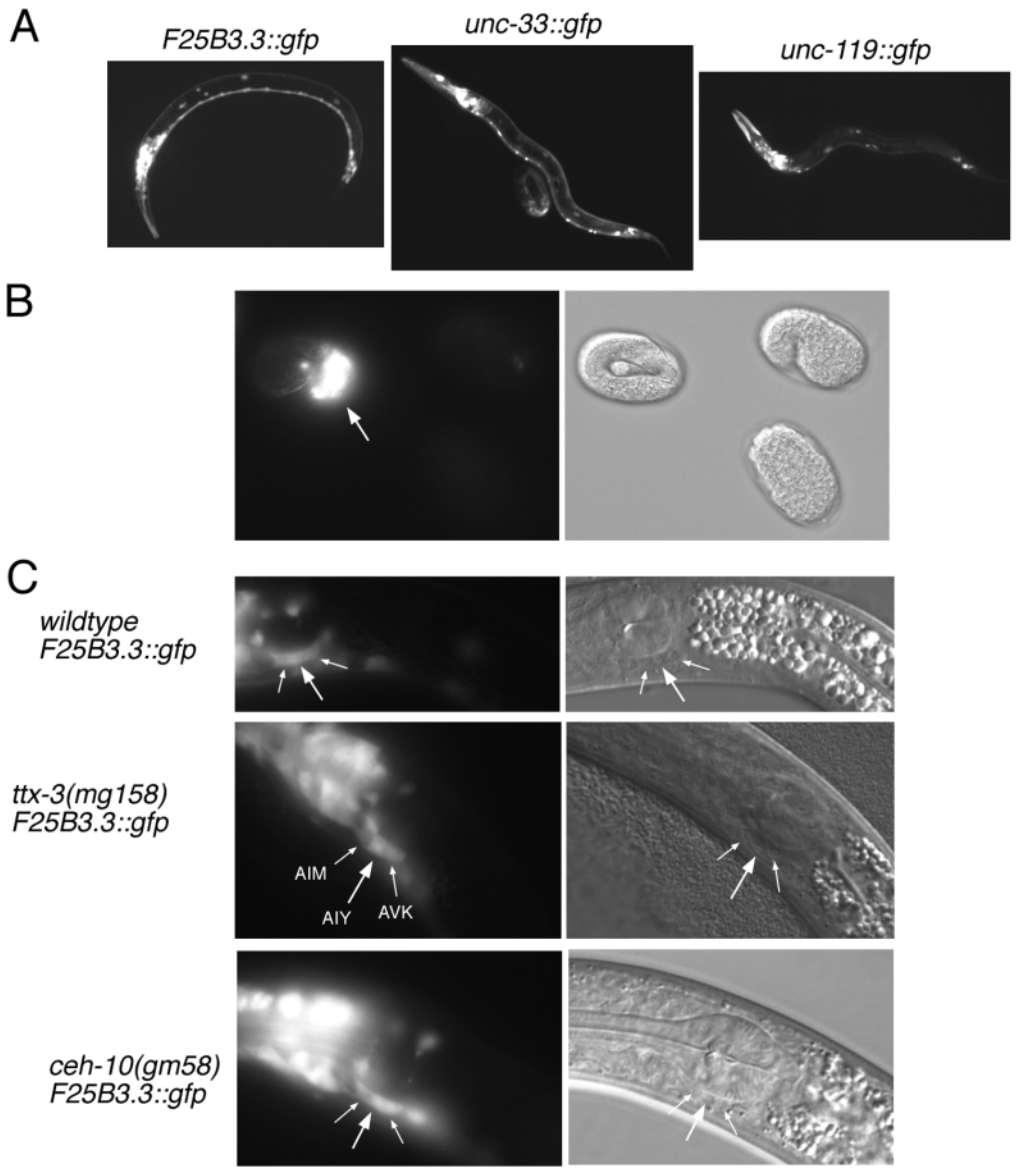

Fig. 6. Examination of pan-neuronal cell fate in *ttx-3* mutants. (A) Expression of three pan-neuronal markers, *unc-119::gfp (otIs45*), *unc-33::gfp (otEx75*) and *F25B3.3::gfp (evIs111),* in wild-type L1 larvae (see also Materials and Methods). (B) F25B3.3::GFP is expressed in postmitotic neurons. Three *evIs111* embryos are shown in a fluorescence micrograph (left panel) and a corresponding DIC micrograph (right panel); the embryos are at the threefold stage (>500 minutes; upper left), the 1.5-fold stage (>400 minutes; upper right) and approximately the 350 minute stage (lower right). Most embryonically generated neurons have been born by the 350 minute stage (Sulston et al., 1983). (C) Expression of pan-neuronal markers in *ttx-3(mg158)* animals. Fluorescence micrographs and the corresponding DIC images are shown side by side. The three white arrows point to the characteristic row of three neurons behind the excretory cell, AIM, AIY and AVK. Animals are late larvae/young adults. 100% *ttx-3(mg158); evIs111* animals showed expression in AIY (*n*=25; large white arrow). Expression of *otIs45* and *otEx75* is mosaic in wild-type animals. 90% of *otIs45* animals show *gfp* expression in AIY (*n*=39); in *ttx-3(mg158);otIs45*, 88% of animals show *gfp* expression in AIY (*n*=48). In *otEx75*, 62% of animals show expression in AIY (*n*=24); in *ttx-3(mg158); otEx75*, 53% of animals show expression in AIY (*n*=28).

tools that monitor aspects of pan-neuronal and non-subtype-specific neuronal differentiation. Besides the previously described *unc-119* gene (Maduro and Pilgrim, 1995), we constructed two other pan-neuronally expressed marker genes, *unc-33::gfp* and *F25B3.3::gfp* (see Materials and Methods). *unc-33::gfp,* like *unc-119::gfp*, marks all neuroblasts and differentiated neurons, while *F25B3.3::gfp* is a marker for all postmitotic neurons (Fig. 6A and Materials and Methods). We crossed each of the three pan-neuronal marker genes into *ttx-3(mg158)* mutant animals and found that loss of *ttx-3* function has no appreciable effect on the expression of any of these marker genes in AIY (Fig. 6C). These findings show that the adoption of subtype-specific characteristics can be separated from the adoption of pan-neuronal characteristics and that *ttx-3* is required for the former but not the latter aspect of AIY development.

As *ceh-10* acts upstream of *ttx-3*, it can be assumed that AIY development is at least as severely affected in *ceh-10* mutants as it is in *ttx-3* mutants. Consistent with this notion we found that several AIY subtype markers failed to be expressed in *ceh-10*-null mutants (Fig. 4 and data not shown). To address whether AIY lost pan-neuronal characteristics in *ceh-10*-null mutants, we examined expression of the *F25B3.3::gfp* pan-neuronal marker in *ceh-10*-null mutants and found it to be unaffected (Fig. 6C). The integrity of AIY generation and positioning in *ceh-10(gm58)* had also been noted previously by DIC microscopy (Forrester et al., 1998). Thus, *ceh-10* and *ttx-3* both act downstream or in parallel to the determination of pan-neuronal cell fate but upstream of the determination of the subtype-specific differentiation program.

Ectopic *ttx-3* expression reveals *ceh-10*-dependent constraints on *ttx-3* function

The results shown above reveal that *ttx-3* is an essential regulator of subtype-specific aspects of the AIY differentiation program. To address whether *ttx-3* is also sufficient to induce AIY-like features in other neurons, we ectopically expressed *ttx-3* throughout the nervous system, using the pan-neuronal

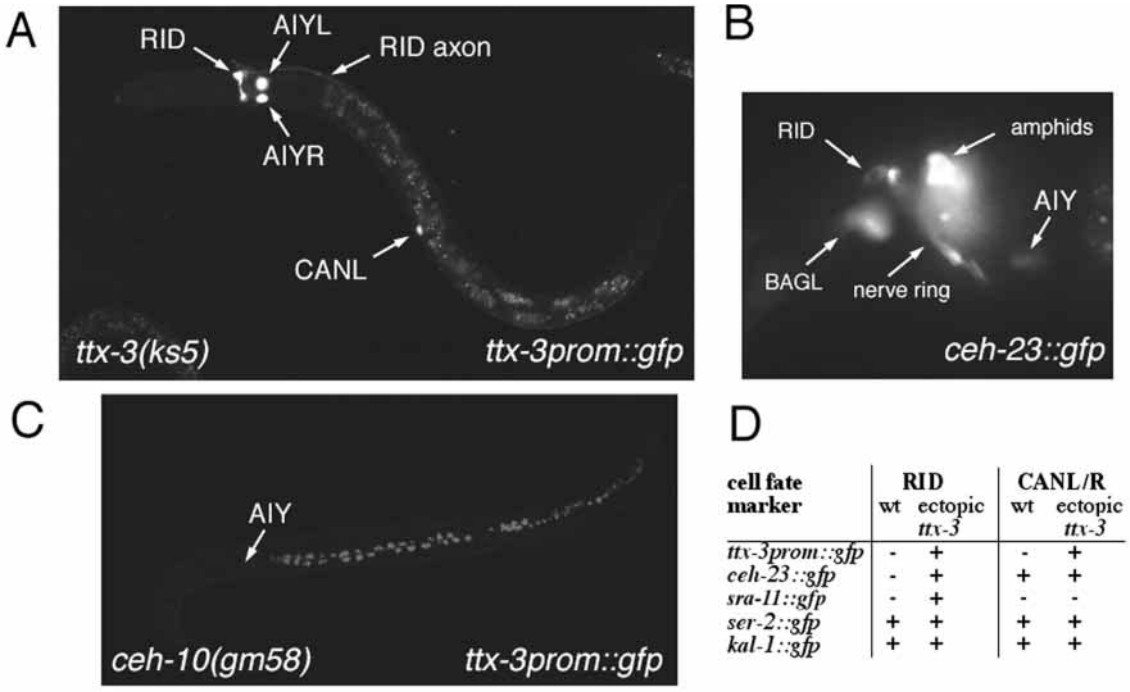

cell fate marker	RID wt	RID ectopic *ttx-3*	CANL/R wt	CANL/R ectopic *ttx-3*
ttx-3prom::gfp	-	+	-	+
ceh-23::gfp	-	+	+	+
sra-11::gfp	-	+	-	-
ser-2::gfp	+	+	+	+
kal-1::gfp	+	+	+	+

Fig. 7. Effects of ectopic *ttx-3* expression and dependence on *ceh-10* activity. (A,B) RID and CAN can adopt AIY-like features upon ectopic expression of *ttx-3*. (A) A transgenic animal is shown that expresses *ttx-3prom::gfp* (normally only expressed in AIY; see Fig. 3B) and *unc-119::ttx-3* from the independently integrated arrays *mgIs18* and *otIs97IV*, respectively, in a *ttx-3(ks5)* background. Note that the autoregulatory defect of *ttx-3prom::gfp* in AIY is completely rescued and that ectopic expression is induced in RID and CAN. The animal is slightly twisted owing to the presence of a *rol-6* injection marker. Ectopic RID and CAN expression could be observed with several independent transgenic lines (see Materials and Methods). (B) Ectopic expression of *ceh-23::gfp* in RID upon pan-neuronal *ttx-3* expression. The genotype of this strain is *kyIs5IV; otEx65*. Eleven out of 14 examined adults show expression in RID. *kyIs5* animals never show GFP expression in RID (n>20). (C) *ceh-10* dependence of ectopic *ttx-3prom::gfp* expression. Homozygous *ceh-10(gm58*) offspring of *ceh-10(gm58)/+; otIs97mgIs18IV* hermaphrodites arrest as L1 larvae and were identified based on their *clr* phenotype. In these animals, no GFP signal can be detected in RID, CAN, or AIY (the approximate position of the AIY interneurons is indicated with an arrow), showing that expression of *ttx-3* from an exogenous promoter can not rescue the *ceh-10(gm58)* phenotype. White dots derive from autofluorescent gut granules. (D) Summary of expression of several AIY cell fate markers in RID and CAN either in wild-type animals or in animals that pan-neuronally express *ttx-3*. Ectopic *sra-11::gfp* expression in RID was observed in 19/19 animals (data not shown) and was never observed in wild-type animals (n>20).

unc-119 promoter (see Materials and Methods). Several independently obtained transgenic *ttx-3(ks5)* mutant animals that express *unc-119::ttx-3* show normal expression of *ttx-3prom::gfp* in the AIY interneurons and are thus rescued for the autoregulatory defect of *ttx-3* expression (Fig. 7). All transgenic lines are viable and show no obvious morphological abnormalities (see Materials and Methods). A pan-neuronally expressed *gfp* reporter construct that visualizes several structural aspects of the nervous system (including presence and localization of axon fascicles; fasciculation within nerve bundles; presence and localization of ganglia) reveals no obvious abnormalities in animals that express *ttx-3* pan-neuronally (data not shown). Intriguingly, *unc-119::ttx-3* transgenic lines behave indistinguishably from wild type in thermotaxis assays, either in the presence or absence of endogenous *ttx-3* gene activity (data not shown); thus, *unc-119::ttx-3* can substitute for loss of endogenous *ttx-3* function but is not sufficient to functionally disrupt other neurons in the thermotaxis circuit.

We tested whether other neurons adopted AIY-like characteristics by examining the expression of five AIY cell fate markers, *ttx-3prom::gfp, ceh-23::gfp, sra-11::gfp, kal-1::gfp* and *ser-2::gfp* in transgenic animals that express *unc-119::ttx-3* (see Materials and Methods). Pan-neuronal expression of *ttx-3* did not lead to a widespread expansion of the expression domains of any of the five markers. However, ectopic expression of the *ttx-3prom::gfp* fate marker could be unambiguously observed in two classes of neurons, the RID motoneuron and the CAN neurons (Fig. 7A). Ectopic expression of the *ceh-23::gfp* marker as well as the *sra-11::gfp* marker could also be detected in RID (Fig. 7B). Ectopic expression of *ser-2::gfp* and *kal-1::gfp* in RID could not be tested, as both markers are already expressed in RID in wild-type animals. Similarly, *ceh-23::gfp, ser-2::gfp* and *kal-1::gfp* are already expressed in CAN in wild-type animals. Hence, RID and CAN already share several characteristics with AIY in wild-type animals, yet *ttx-3* is able to confer even more AIY-like characteristics to these cells upon ectopic expression (Fig. 7D). However, the axonal morphology of RID and CAN is not obviously affected by ectopic *ttx-3* expression (Fig. 7A and data not shown); thus, *ttx-3* is capable of imposing only a subset of the AIY differentiation program on the RID and CAN neurons. We conclude that the activity of *ttx-3* is highly constrained by the presence of other regulatory factors, and that only in certain contexts does *ttx-3* have the capacity to partially re-program neural differentiation.

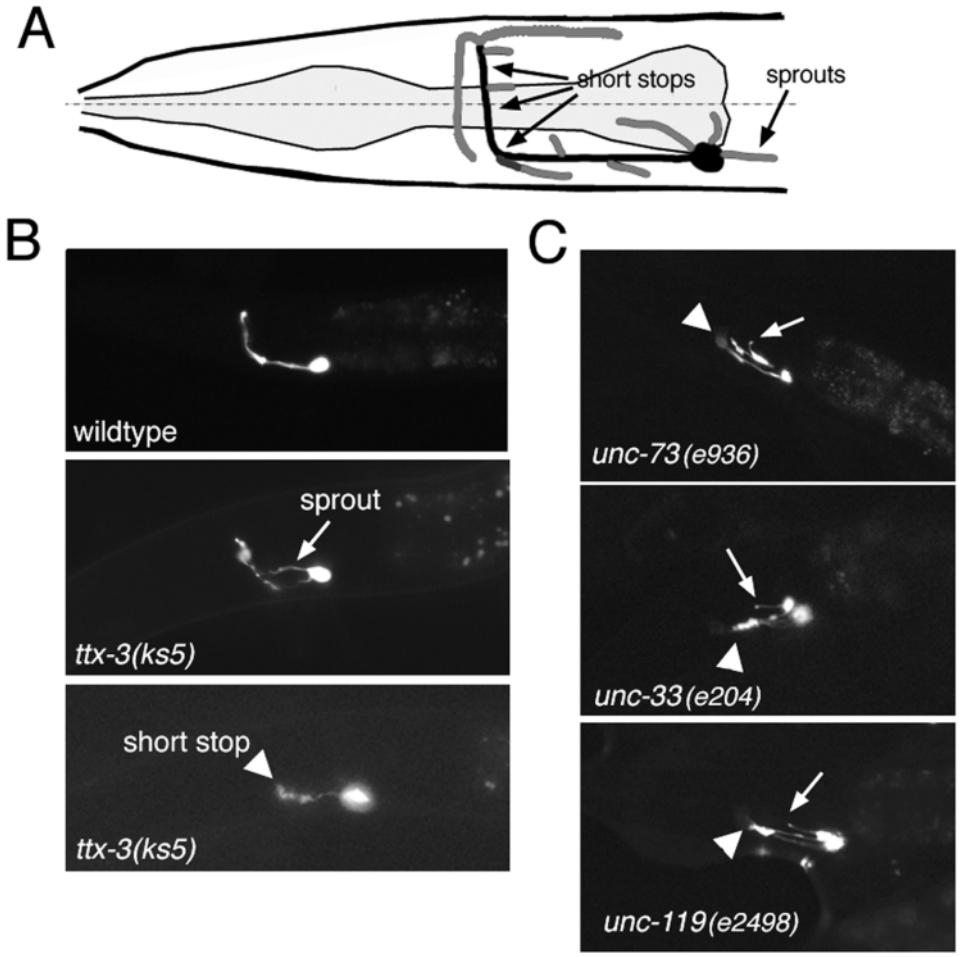

Fig. 8. Characterization of the neuroanatomical defects in *ttx-3* mutant animals. (A) Axonal defects observed in various mutants. The wild-type AIY axon is shown in black. In wild-type animals, a short process (shown in dark gray) can occasionally be observed in the region where the main axon turns dorsally to enter the nerve ring; those are not scored as a mutant phenotype, unless they are longer than 10 μm (shown as light gray addition to the dark gray line). Schematic examples of aberrant axon sprouts are in light gray. We set the minimum length for scoring aberrant sprouts that emanate from the axon arbitrarily at 2 μm. As cell bodies occasionally narrow into a thin ending, we arbitrarily set the criteria to score sprouts from the cell body more stringently at 4 μm. Occasional 'splits' of the axon in the nerve ring region are counted as sprouts. Small enlargements along the axon, rarely observed in wild-type animals, often observed in pathfinding mutants, are not scored as sprouts. Every case in which the main axon does not meet the axon of its contralateral homolog at the dorsal midline is classified as 'short stop'; the main axon stalls either at the turning point into the nerve ring (but never before that point), or at various points below or above the dorsoventral midline (black arrows). (B) Characteristic examples of axonal defects observed in *ttx-3* mutants. AIY is visualized with *mgIs18*. Quantitative data are shown in Table 3. Similar results have also been obtained with several extrachromosomal *ttx-3prom::gfp* lines (Hobert et al., 1997). For this analysis we could make use only of the *ttx-3(ks5)* allele because, owing to the more severe reduction of *ttx-3prom::gfp* expression in the stronger *ttx-3* alleles, the axon of the AIY interneurons cannot be visualized. It is thus possible that in the stronger alleles AIY neuroanatomy is even more strongly affected. (C) Representative examples of AIY neuroanatomy in *unc-33(e120)*, *unc-73(e936)* and *unc-119(e2498)* mutant animals, visualized with *mgIs18*. White triangles point to short stops, white arrows to sprouts. Animals shown in this figure are late larvae and young adults. Notably, besides the short-stop defect of the main axon of the AIY neurons, these axon pathfinding mutants also cause axon sprouting defects. As neural activity defects do not cause axon sprouting in AIY (Table 3), the axon sprouting observed in pathfinding mutants are unlikely to be a secondary consequence of aberrant connectivity caused by aberrant pathfinding. We rather hypothesize that the axon sprouting defect observed in pathfinding mutants as well as in *ttx-3* mutants reflects an inability of the neuron to initiate and maintain the proper outgrowth of a single, monopolar axon.

Notably, the only two neuron classes in which AIY-like characteristics could be induced by pan-neuronal *ttx-3* expression, RID and CAN, normally express *ceh-10* (Fig. 1), suggesting that it is the presence of *ceh-10* that constrains ectopic *ttx-3* activity to these neurons. We tested this hypothesis by examining ectopic *ttx-3prom::gfp* expression in RID and CAN in animals that carry an integrated *unc-119::ttx-3* expressing array, but lack *ceh-10* function. We found that in these animals *ttx-3prom::gfp* expression is downregulated or completely turned off in RID, CAN and AIY (Fig. 7C). This observation points to a requirement of *ceh-10* for *ttx-3*-dependent regulatory events. The mere co-existence of *ceh-10* and *ttx-3* is however not sufficient to confer AIY-like characteristics to a neuron, as pan-neuronal misexpression of *ttx-3* does not appear to induce the expression of AIY-like characteristics in other *ceh-10*-expressing cells (such as RMED, AIN etc.; data not shown). We conclude that *ttx-3* is able to regulate the expression from its own promoter and of presumptive target gene promoters only in particular cellular contexts, which are directly or indirectly dependent on the presence of the *ceh-10* homeobox gene.

ttx-3 is also implicated in axon outgrowth and pathfinding

Our identification of genes whose expression depends on *ttx-3* function represents one route to assess the impact of *ttx-3* on AIY differentiation. Another approach is to find genes whose mutant phenotype is similar to the *ttx-3* mutant phenotype and whose function may hence be related to *ttx-3* function. We have previously shown that the AIY interneurons display a characteristic set of neuroanatomical defects in *ttx-3* mutant animals. These defects included inappropriate termination of the main axon and sprouting of additional neurites (Hobert et al., 1997; see also Fig. 8). Recently, ectopic neurite sprouting in *C. elegans* was described as a secondary consequence of defects in neuronal activity of sensory neurons and

Table 3. Axon morphology of the AIY interneuron class in defined mutant backgrounds

Genotype		Animals with short stop (%)	Animals with sprouts (%)	*n*
Wild type (*mgIs18*)	Adult	3	2	104
*ttx-3(ks5)**	L1	14	44	55
	L2	20	52	59
	L3	28	49	57
	L4	22	55	76
	Adult	18	51	67
Sensory mutants‡				
daf-6(e1377), che-3(e1124), che-11(e1810), osm-6(p811), tax-2(p691), tax-4(p678)		<2	0	>45
Synaptic transmission mutants‡				
unc-64(e246), unc-18(e81), unc-13(e51,e1091,s69), aex-3(n2166), rab-3(js49), unc-31(e928), unc-104(rh43), snb-1(md247, js124), flp-1(yn2), unc-17(e245), unc-7(e5)		<3	1	>50§
Membrane potential and Ca^{2+} signaling				
unc-36(e251), unc-2(mu74), egl-36(n728), egl-19(ad695gf), egl-19(n2368gf), eat-6(ad467)		<3	<2	>48
Axon outgrowth and pathfinding mutants¶				
Intracellular				
unc-33(e204)	(CRMP)	53	25	80
unc-44(e362)	(ankyrin)	61	61	74
runc-51(e369)	(Ser/Thr kinase)	4	11	115
unc-53(e404)		32	3	119
unc-73(e936)	(rho/rac GRF)	70	17	78
unc-76(e911)	(FEZ1)	97	33	103
unc-115(mn481)	(LIM domains)	3	2	67
unc-119(e2498)		100	46	63
Transmembrane/secreted				
sax-3(ky123)	(Robo)	90	49	91
vab-1(dx31)	(Eph-R)	0	6	66
unc-40(e1430)	(Netrin-R)	7	14	81
unc-5(e53)	(Netrin-R)	1	7	114
unc-6(ev400)	(Netrin)	23	12	71
ina-1(gm144)	(α-Integrin)	92	16	98
Others**				
unc-43(n498gf)	(CamKII)	0	0	47
unc-43(e408lf)		0	0	88
sax-2(ot10)		0	55	67
lin-12(n941)	(Notch)	3 (0%)	4 (5%)	103 (41)‡‡

AIY neuroanatomy was scored in adult animals using the integrated *ttx-3prom::gfp* array *mgIs18* if not indicated otherwise; the scoring criteria are detailed in Fig. 8A. Percentages refer to the number of animals in a population with a given defect; defects of >10% penetrance are shaded. References for mutants can be found elsewhere (Antebi et al., 1997; Culotti, 1994; Rand and Nonet, 1997).

**ttx-3prom::gfp* marker gene expression, which visualizes AIY neuroanatomy, is too low in *ttx-3* null mutants; thus, we could only test the hypomorphic *ks5* allele (see Fig. 3B).

‡*tax-2(p671), tax-4(p678), unc-31(e928), unc-7(e5), flp-1(yn2)* and *snb-1(js124)* are null mutants, the other alleles are strong loss-of-function alleles. Note that several of those strong, yet non-null alleles have been found to cause axon sprouting in motoneurons (Zhao and Nonet, 2000).

§*unc-13(e51)* and *unc-18(e81*) have each been examined with two independent *ttx-3prom::gfp* integrants, *mgIs18* and *mgIs32* to exclude strain background artifacts. The *unc-13(e51)* allele (strain name: RM2423) is a four times back-crossed derivative of the canonical *unc-13(e51)* strain CB51 and was kindly provided by J. Rand. CB51 contains a linked *unc-122* mutation in the background (Richmond et al., 1999), which is absent in RM2423. 18 animals were scored for the *snb-1* null allele *js124* (a gift from Mike Nonet), which die as L1s.

¶Most of the alleles shown in this category are null alleles.

**This category includes mutants shown to cause axon sprouting in other contexts, such as *sax-2*, which causes sensory axon sprouting in *C. elegans* (Zallen et al., 1999), CamKII, which regulates axon sprouting in *C. elegans* and in the frog optic tectum (Wu and Cline, 1998; Zallen et al., 1999) and *Notch*, which regulates sprouting in the cerebellar cortex (Sestan et al., 1999) and axon pathfinding in the fly CNS (Giniger et al., 1993). *sax-2(ot10)III* is a newly identified allele of the previously described *sax-2* gene (Z. A.-G. and O. H., unpublished).

‡‡This result differs from a recent report that showed AIY axon morphology defects in *lin-12(n941)* mutants (Wittenburg et al., 2000). We examined AIY morphology in the *lin-12(n941)* null mutant using either of two independently generated *ttx-3prom::gfp* integrants, *mgIs18* or *mgIs32* (numbers shown in parenthesis). *lin-12(n941); mgIs18* and *lin-12(n941)mgIs32* were each balanced with the *lin-12* rescuing array *arEx29* (Fitzgerald et al., 1993). AIY anatomy was scored in animals that had lost the balancing *arEx29* array, and hence were non-rolling and had a large blip at the vulva. Similar results were obtained when *lin-12(n941)* was balanced with a *lin-12(+)* chromosome (data not shown). We never observed any of the severe axonal defects reported recently in any of the strains (Wittenburg et al., 2000). In contrast to Wittenburg et al., we also did not observe AIY axonal defect in *sel-12*/presenilin mutants (using a newly isolated null allele of the *sel-12* presenilin gene; I. Temkin and I. Greenwald, personal communication) or in *egl-19(n2368gf)* mutants; additionally, no defects could be observed in another *egl-19* gain-of-function allele or in any other synaptic transmission/electrical activity mutant shown in the Table. As we observed axonal defects of AIY in several defined genetic backgrounds (as shown in the Table; H. Buelow, K. Berry and O. H., unpublished) with either of two independently integrated reporter gene arrays, as well as with extrachromosomal arrays, the presence of any linked suppressor mutations in our strain backgrounds can be excluded. As Wittenburg et al. used distinct *ttx-3prom::gfp* extrachromosomal arrays for the observation of AIY defects and for their rescue experiments, it cannot be excluded that the effects that they observe are due to a partial defectiveness differentially induced by distinct *ttx-3prom::gfp* arrays (notably, the morphology of AIY looks irregularly shaped in a wild-type animal that expresses a *ttx-3prom::gfp* array; Wittenburg et al., 2000) and/or due to mutations in their strain background.

motoneurons (Peckol et al., 1999; Zhao and Nonet, 2000). In contrast to their capacity to induce sprouting in motoneurons (Zhao and Nonet, 2000), we found that the synaptic transmission mutants *unc-18(e81)* and *unc-13(e51)*, and the neurotransmitter transport mutant *unc-17(e245)* have no effect on AIY axon morphology (Table 3). Similarly, several other tested neurotransmission mutants also do not cause any neuroanatomical defects in AIY (Table 3). We additionally tested the outcome of electrical silencing of AIY by individually expressing two gain-of-function K^+ channel mutant subunits, EGL-36 (E142K, P489S) (Johnstone et al., 1997) and EGL-2 (A478V) (Weinshenker et al., 1999) under the control of an AIY-specific *ttx-3* promoter fragment and found no effect on AIY neuroanatomy (data not shown).

Furthermore, sensory activity mutants that cause neurite sprouting in sensory neurons, such as *tax-2*, *tax-4*, *eat-6*, *che-3* and others (Peckol et al., 1999) have no effect on AIY axon morphology (Table 3). Additionally, while neuronal-activity dependent axon sprouting of sensory neurons and motoneurons has recently been shown to be strongly influenced by ambient temperature and the developmental stage of the animal (Zhao and Nonet, 2000; Peckol et al., 1999; P. Loria and O. H., unpublished), we found no impact of these parameters on the *ttx-3(ks5)* induced sprouts (Table 3; data not shown).

Taken together, unlike the situation in defined sensory and motoneurons, the absence of synaptic transmission is unlikely to account for the neurite sprouting defects in *ttx-3* mutant animals. We favor the possibility that the axonal defects observed in *ttx-3* mutant animals represent developmental defects during the phase of axonal outgrowth. To test this notion, we compared the qualitative appearance and penetrance of axonal sprouts observed in several axon pathfinding mutants with those seen in *ttx-3(ks5)* mutants (*ks5* is the only allele that allows visualization of AIY neuroanatomy; Fig. 3). We found that mutations in almost all of the intracellularly acting outgrowth/pathfinding proteins, which are thought to act throughout the nervous system (Antebi et al., 1997; Culotti, 1994; Hedgecock et al., 1985; McIntire et al., 1992), show defects that resemble those seen in *ttx-3* mutants (Fig. 8; Table 3). Furthermore, we found that mutations in the cell-specific axon guidance cues *unc*-6/Netrin (Hedgecock et al., 1990), *sax-3*/Robo (Zallen et al., 1998) and *ina-1*/Integrin (Baum and Garriga, 1997), but not in *vab-1*, the only ephrin receptor in *C. elegans* (George et al., 1998), or in *lin-12*/Notch (Giniger et al., 1993; Greenwald et al., 1983) cause axonal defects in the AIY interneurons (Table 3). This is an intriguing finding, as *unc-6, sax-3* and *ina-1* have not been previously implicated in axon outgrowth into the nerve ring. *unc-6* null mutants show normal guidance of amphid sensory axons in the nerve ring (Hedgecock et al., 1990), *ina-1* hypomorphic mutants show fasciculation defects, but no apparent outgrowth defects of sensory axons in the nerve ring (Baum and Garriga, 1997) and *sax-3* null mutants were reported to show displacements of the nerve ring, but only subtle and cell type-specific premature termination of nerve ring axons (Zallen et al., 1999). The impact of *unc-6, sax-3* and *ina-1* on AIY axon outgrowth in the nerve ring is thus unlikely, owing to the disruption of nerve ring pioneer neurons because that would presumably cause more pleiotropic axon outgrowth defects in the nerve ring. The netrin, robo and integrin guidance systems may act directly in the AIY interneuron class. Whether components of these guidance systems are under direct control of the TTX-3 homeodomain protein remains to be investigated.

Given the similarity in phenotypes observed between axon outgrowth/pathfinding mutants and *ttx-3* mutants, we hypothesize that *ttx-3* is required to regulate correct axon outgrowth and pathfinding of the AIY interneurons. As *ttx-3* appears to have no effect on the expression of pan-neuronal characteristics (Fig. 6), we hypothesize that cell-type specific aspects of AIY axon outgrowth, such as the expression of a guidance receptor, rather than pan-neuronal aspects of axogenesis, are affected in *ttx-3* mutants.

Role of *ttx-3* in the differentiation of other neuron classes

In contrast to its pronounced effect on AIY interneuron differentiation, *ttx-3* does not appear to influence the adoption of several subtype-specific differentiation features of the *ttx-3*-expressing sensory neuron classes ADL and ASI. The expression of five differentiation markers of the ASI sensory neurons (*daf-7::gfp, osm-10::gfp, sre-1::gfp, zig-2::gfp* and *zig-3::gfp*) was unaffected in *ttx-3(mg158)* mutants (Table 2). Similarly, the ADL sensory neurons still expressed the putative odorant receptors *srb-6* and *sre-1* in the absence of *ttx-3* activity (Table 2). Both ADL and ASI are also still capable of being filled with the vital dye DiI in *ttx-3* mutant animals, suggesting that these sensory neurons do not require *ttx-3* to assemble intact, exposed sensory endings.

We examined the fate of the AIA interneuron class in *ttx-3* mutants and found that expression of the only two known marker genes of AIA fate are partially affected. *sra-11::gfp* expression from the *otIs62* array can be observed in 64% of *ttx-3(+)* animals (n=45) and 38% (n=70) of *ttx-3(mg158)* animals (Fig. 5); UNC-17 antibody staining in AIA can be observed in 94% of wild-type animals (n=32) and 66% (n=58) of *ttx-3(ks5)* mutant animals (a *ttx-3(ks5); mgIs18* strain was used, which in contrast to the stronger *ttx-3* alleles permits an unambiguous identification of the AIA neurons by co-staining with anti-GFP antibodies). Additionally, the AIA interneurons appear to display neuroanatomical defects (data not shown). Further cell fate markers and functional assays for the AIA interneurons need to be established in order to fully assess the impact of *ttx-3* on AIA differentiation and function.

Regulatory relationship between *ceh-10, ttx-3* and *ceh-23* in other neurons

Based on reporter gene analysis, the AIY interneuron class appears to be the only neuron class in which the expression of the three homeobox genes *ceh-10, ttx-3* and *ceh-23* overlaps. The otherwise largely non-overlapping expression pattern of these genes illustrates that *ceh-10* is neither sufficient to turn on *ttx-3* expression in other neuron classes (RMED, RID, CEP, ALA, AVJ, AIN or CAN) nor necessary to turn on *ttx-3* expression in the ADL, ASI or AIA neuron classes. In addition, *ttx-3* is neither sufficient to turn on *ceh-23* expression in ASI or AIA nor necessary to turn on *ceh-23* expression in several other sensory neuron classes (Fig. 1C). However, there are two neuron classes in which the expression of two of the three homeobox genes overlaps (ADL, *ttx-3* and *ceh-23*; CAN, *ceh-10* and *ceh-23*), thus raising the question whether the regulatory relationship between these genes, observed in the AIY interneuron, also exists in ADL and CAN. We found that

ceh-23 expression in ADL was unaffected in *ttx-3(mg158)* mutant animals (data not shown). Thus, the regulatory relation between *ttx-3* and *ceh-23* is not conserved in neurons other than the AIY interneuron class. In contrast, in the CAN neurons, in which *ceh-10* expression overlaps with *ceh-23* expression, *ceh-10* regulates *ceh-23* expression (Forrester et al., 1998). However, this regulation is independent of *ttx-3* which is not expressed in CAN. Accordingly, *ceh-23* expression in CAN is unaffected in *ttx-3(mg158)* mutant animals (data not shown). Thus, a regulatory relationship between these three homeobox genes exists in one neuron class (AIY), partially in another neuron class (CAN) and not at all in another neuron class (ADL).

DISCUSSION

We have described here a regulatory cascade of three transcription factors which are involved in controlling AIY interneuron differentiation (Fig. 9). All three transcription factors are expressed and appear to function after the terminal cell division that generates the AIY interneuron class. *ceh-10* and *ttx-3* determine all known aspects of subtype-specific AIY interneuron fate while *ceh-23* ensures maintained expression of one AIY differentiation feature (Fig. 9). While transcriptional regulatory cascades have previously been described in several developmental contexts in the nervous system (Anderson and Jan, 1997; Jurata et al., 2000), they have only rarely been identified in postmitotic neurons and the absence of appropriate cell fate markers has usually precluded an in-depth analysis of the role of transcription factor cascades in the differentiation of defined neuron classes. It is presumably the complexity of these postmitotically acting transcriptional networks that translates cell lineage history and environmental cues into the generation of the enormous variety of cell types in the nervous system.

Role of *ceh-10* in AIY development

As *ceh-10* regulates *ttx-3*, which in turns regulates all known aspects of AIY development and function, it is not immediately apparent what distinguishes the function of *ceh-10* and *ttx-3*. As *ceh-10* is only expressed embryonically, whereas *ttx-3* and all its target genes are expressed embryonically and post-embryonically, we consider it unlikely that *ceh-10* and *ttx-3* act strictly together as co-factors on both the *ttx-3* promoter and then, subsequently, the target gene promoters. However, it can not be the only role of *ceh-10* to initiate *ttx-3* gene expression that then serves to regulate its own expression, as expression of *ttx-3* under control of the pan-neuronal, and presumably non-*ceh-10*-dependent *unc-119* promoter is not able to induce expression from the *ttx-3* promoter in the AIY interneurons in *ceh-10* null mutant animals. Also, ectopic *ttx-3* is not sufficient to induce expression from its own promoter in non-*ceh-10*-expressing neurons. *ceh-10* thus appears to provide means to allow the TTX-3 protein to regulate its own expression; one out of several possible scenarios is that *ceh-10* initiates the expression of yet another transcription factor(s) that acts together with TTX-3 to regulate expression from the *ttx-3* promoter and possibly other target gene promoters. In addition to its role in regulating *ttx-3* expression, *ceh-10* could be involved in the regulation of other as yet unknown and *ttx-3*-independent AIY differentiation characteristics.

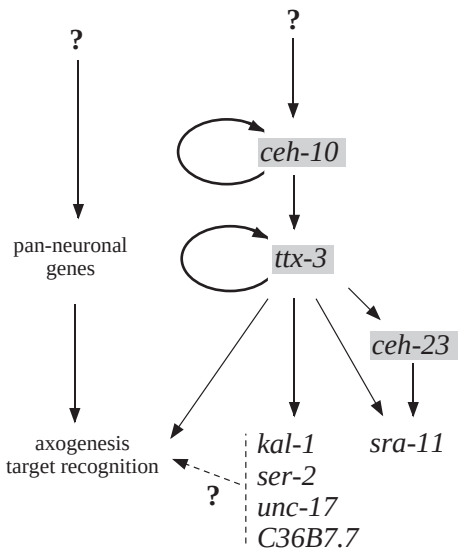

Fig. 9. Model for transcriptional regulatory events in the AIY interneurons. We propose that CEH-10 activates the expression of the TTX-3 protein, which then – either in conjunction with CEH-10 or other as yet unknown transcription factors – activates the expression of *ceh-23* and other target genes. TTX-3 and CEH-23 presumably both contribute to the regulation of *sra-11* expression. Pan-neuronal features are determined either upstream or in parallel to the *ceh-10→ttx-3→ceh-23* cascade. Regulatory events that determine pan-neuronal and cell-type specific features of AIY (via *ceh-10/ttx-3/ceh-23*) are unknown and are denoted by a question mark. Based on their prominent roles in neuronal patterning in several systems, we tested whether the *C. elegans* Pax-6/Eyeless homolog *vab-3* (Chisholm and Horvitz, 1995), the *C. elegans* homolog of MATH1/Atonal, *lin-32* (Zhao and Emmons, 1995) and the *C. elegans* NeuroD homolog *cnd-1* (Hallam et al., 2000) couple early embryonic patterning events to the transcriptional regulatory cascade of *ceh-10, ttx-3* and *ceh-23* in AIY and found this not to be the case (data not shown). It is conceivable that some of the TTX-3 target genes shown here (*ser-2, sra-11, C36B7.7, kal-1)* are directly involved in axonal defects observed in *ttx-3(ks5)* mutants; this possibility is denoted by a broken arrow. Isolation of mutations in these genes will address this issue. Although *unc-17* hypomorphic mutants do not show axonal defects, it is possible that cholinergic transmission contributes together with other genes to axogenesis of AIY (Table 3). At this point it is not clear whether any of the regulatory events that involve CEH-10, TTX-3 and CEH-23 depend on direct interaction of the respective homeodomain protein with the promoter of the presumptive target gene. Within the *ttx-3* promoter we have defined two motifs of 5bp and 7bp length, spaced by 20 nucleotides, which are both necessary for the activity of the promoter; both elements contain a variant of the core homeodomain binding site (A. Wenick and O. H., unpublished). Similar clustered motifs can be found in other presumptive TTX-3 target gene promoters. We speculate that these motifs may represent binding sites for TTX-3 and possible co-factor(s). *ceh-10* autoregulation has been demonstrated by Forrester et al., 1998.

ttx-3 is a key regulator of AIY interneuron differentiation

The understanding of the function of Lhx genes in neuronal development has in many instances been hampered by a lack of molecular markers, which precluded the precise assessment

of the consequences of absence of Lhx gene function. By establishing a set of AIY differentiation markers and by visualizing axon morphology using a single neuron class-specific marker, we have carried out a detailed characterization of the consequences of loss of *ttx-3* function. In *ttx-3* mutants, expression of all known AIY cell fate markers is severely affected; moreover, the neuroanatomical defects of AIY in *ttx-3* mutants resemble the defects seen in axonal pathfinding mutants. We conclude that *ttx-3* is required to determine most, if not all subtype-specific aspects of the developmental program of the AIY interneurons, including the expression of its neurotransmitter phenotype (*unc-17* expression), potential neurotransmitter receptors (*ser-2*), secreted signaling or adhesion proteins (*kal-1, C36B7.7*), proteins of unknown function (*sra-11*) and aspects of axonal outgrowth (Fig. 9). The maintained expression of *ttx-3* throughout the life of an animal suggests that *ttx-3* is continuously required to maintain differentiated features of the AIY interneurons and it is thus possible that *unc-17, ser-2, sra-11, kal-1* and *C36B7.7* are direct targets of the TTX-3 protein. We are in the process of testing TTX-3 binding to the promoters of these genes using *in vitro* DNA binding assays.

In spite of its prominent role in determining subtype-specific neuronal features, TTX-3 does not determine pan-neuronal characteristics. This can be inferred from the neuron-like appearance of AIY in *ttx-3* mutant animals (e.g. the AIY cell body extends an axon projection towards the nerve ring) and from the observation that the expression of three pan-neuronal markers is unaffected in *ttx-3* mutants. These findings show that adoption of pan-neuronal features is separable from the adoption of more cell-type restricted features, and show that *ttx-3* genetically separates these two aspects of neuronal differentiation.

Although *ttx-3* is required in AIY to adopt all of its known cell-type specific characteristics, *ttx-3* is not sufficient to impose a complete AIY differentiation program onto other neurons. Although ectopic *ttx-3* expression can induce the adoption of several AIY-like characteristics, it can only do so in two neuron classes (RID and CAN) and even in those cases *ttx-3* is not capable of conferring AIY-like structural features (cell position, axonal anatomy) onto these neurons. It is presumably the absence of an appropriate transcription factor 'code' (discussed below) that does not allow TTX-3 to confer AIY-like features to more than two other neuron classes and to more completely convert RID and CAN to an AIY-like fate. Such context-dependent restrictions of Lhx gene action have also been observed for the *Drosophila Islet* gene and the *C. elegans mec-3* gene. *Islet* is necessary for expression of the dopaminergic and serotonergic phenotype of several ventral cord neurons, yet it is not sufficient to induce serotonergic phenotypes upon ectopic expression and is sufficient to induce dopaminergic phenotypes in only a small set of neurons (Thor and Thomas, 1997). Ectopic expression of the Lhx gene *mec-3*, which is required to determine touch neuron fate, induces expression of a touch neuron marker in only one to 16 extra cells, all of which appear to contain a homeodomain protein, UNC-86, which acts together with MEC-3 in touch neurons (Duggan et al., 1998). The presence of UNC-86 may thus impose a requirement for ectopic MEC-3 activity that is comparable to the requirement of CEH-10 for ectopic TTX-3 activity.

ttx-3 does not appear to play a central role in the differentiation programs of other neurons besides AIY and possibly AIA. The expression of all tested differentiation markers of two types of sensory neurons that normally express *ttx-3* is intact in *ttx-3* mutants. Moreover, these sensory neurons appear structurally unaffected by loss of *ttx-3* function. This is in striking contrast to AIY, in which the expression of all tested differentiation markers as well as axonal anatomy is severely affected in *ttx-3* mutants. We thus consider it most likely that *ttx-3* exerts a different regulatory impact in the cell fate specification of these sensory cell types. Owing to the absence of molecular markers as well as functional assays, the role of *ttx-3* in AIA interneuron differentiation is unclear at this point. As the expression of the *sra-11* and *unc-17* fate markers is partly affected and as the AIA neurons appear to display anatomical defects in *ttx-3* mutants, it is possible that *ttx-3* is as crucial a differentiation regulator in AIA as it is in AIY.

Function of *ceh-23* in AIY differentiation

sra-11, an orphan seven-transmembrane-receptor of unknown function, is most strongly expressed in the AIY and AVB neuron classes in L1 larvae, yet consistent and strong expression persists throughout adulthood in the AIY, but not the AVB neuron class. We have shown here that this AIY-specific maintenance mechanism requires *ceh-23* gene activity. In contrast, the initiation of *sra-11* expression requires *ttx-3* but not *ceh-23* activity. It is tempting to speculate that separable initiation and maintenance mechanisms introduce an additional level of regulation that could be subject to dynamic control. For example, CEH-23 protein activity could be post-transcriptionally regulated to allow for subtle and environmentally controlled changes in *sra-11* expression during the life time of an animal.

The analysis of the role of *ceh-23* and *sra-11* in regulating aspects of AIY function will have to await a more complete understanding of the processes in which the AIY interneuron participates. While *ceh-23*, and hence the maintenance of *sra-11* expression, appear to have no impact on the function of AIY in processing thermosensory information, the complex patterns of synaptic connectivity of the AIY interneurons (White et al., 1986) suggest as yet unknown roles of AIY in processing and integration of various other types of sensory information. *ceh-23* and *sra-11* may have a role in determining these unknown aspects of AIY function.

Gene regulatory interactions strongly depend on cellular context

The regulatory cascade of three homeobox genes and their target genes that we defined in the AIY interneurons shows intriguing aspects of both conservation and non-conservation in other neuron classes. Previously, Forrester et al., have shown that *ceh-10* regulates *ceh-23* in both AIY and CAN (Forrester et al., 1998). We show that in AIY this regulatory influence is exerted via *ttx-3*; however, in CAN, the impact of *ceh-10* on *ceh-23* expression is independent of *ttx-3* (inferred from both a lack of detectable *ttx-3* expression in CAN and persistent *ceh-23* expression in CAN in *ttx-3* mutants). *ceh-10* may induce the expression of a transcription factor in CAN that functions in *ceh-23* regulation in an analogous fashion to *ttx-3* in AIY. Adding to the complexity, the ADL sensory neuron class co-expresses *ttx-3* and *ceh-23*, yet *ttx-3* has no

effect on *ceh-23* expression in ADL (unlike in AIY). Taken together, the promoter of the *ceh-23* gene is likely to contain regulatory elements that are used differentially in distinct tissue types.

The largely non-overlapping patterns of expression of *ceh-10, ttx-3* and *ceh-23* and their complex patterns of regulatory relationship argue that none of these transcription factors alone is sufficient to impose specific differentiation aspects entirely on their own and thus point to a highly context-dependent co-factor requirement of each of these factors. Our findings illustrate the complexity of transcriptional regulation in the nervous system, and in particular, the complexity of interdependence of transcription factor action.

The context-dependent regulation of gene expression exemplified with the *ceh-10, ttx-3* and *ceh-23* cascade can also be illustrated at the level of the target genes of this transcription factor cascade, which is particularly intriguing as these are function genes that determine the individual properties of a neuron. For example, expression of the vesicular acetylcholine transporter UNC-17 marks the entire set of cholinergic neurons in *C. elegans*, which consists of at least 22 different neuron classes (Alfonso et al., 1993; Rand and Nonet, 1997). *unc-17* gene expression is under control of TTX-3 exclusively in the AIY interneurons (and partly in AIA), and hence its expression must be controlled in a 'piece-meal' fashion by different transcription factors in different cholinergic cell types. Either the *unc-17* promoter contains a transcription factor-binding site that is used by similar, yet differentially expressed members of a transcription factor class (e.g. a homeodomain-binding site that is used by homeodomain proteins that are present in distinct subsets of cholinergic neurons), or the *unc-17* promoter displays a complex and highly modular structure that integrates different transcription factor inputs in distinct cholinergic cell types. Interestingly, cell-specific regulation of a neurotransmitter phenotype has also been described for the *ttx-3* ortholog *apterous* in *Drosophila*. The *Drosophila* FMRF-NH_2 neuropeptide gene is expressed in 44 neurons of the fly CNS, eight of which co-express *apterous*; in those eight cells FMRF-NH_2 gene expression is under control of *apterous*, which in turn is expressed in about 100 CNS neurons (Benveniste et al., 1998). Thus, *apterous* is only required for FMRF-NH_2 gene expression in a highly cell type-specific context.

C. elegans LIM homeobox genes: cell fate loss versus cell fate switch and transcription factor codes

The mutant phenotype of *ttx-3* shows striking similarities and dissimilarities with the mutant phenotypes of other Lhx genes in *C. elegans*. In *mec-3* mutant animals, touch sensory neurons have lost most if not all cell type-specific mechanosensory differentiation features, yet retain neuron-like features (Chalfie and Sulston, 1981; Duggan et al., 1998; Way and Chalfie, 1988), a phenotype that resembles the *ttx-3* mutant phenotype described here. In contrast, *lim-6* does not appear to be required for expression of most cell type-specific characteristics in a defined motoneuron and an interneuron (Hobert et al., 1999; O. Aurelio, and O. H., unpublished). The case appears more different with the *C. elegans* ortholog of the *lhx6/8* subclass of Lhx genes, *lim-4*. In the absence of *lim-4* function one class of cells that normally expresses *lim-4*, the AWB sensory neuron class, switches its fate in both structural and functional terms to that of another type of sensory neuron, the AWC class (Sagasti et al., 1999). Although it is possible that the AIY neurons switch fate in *ttx-3* mutants, we rather interpret the loss of cell fate marker gene expression, the abnormal appearance of AIY and our failure to find ectopic marker gene expression as indication of a loss of cellular differentiation that is not necessarily accompanied by a cell fate switch.

These examples of differences of Lhx gene mutant phenotypes, i.e. complete loss of differentiation program (*ttx-3*), partial loss of differentiation program (*lim-6*) and a binary switch in differentiation program (*lim-4*) cannot, however, be taken as evidence for a specialization of function of members of specific Lhx subclasses. For example, while *ttx-3* presumably affects the complete differentiation program of AIY, we found no obvious impact of *ttx-3* on sensory neuron differentiation. Additionally, while loss of *lim-6* only partially affects the differentiation program of an interneuron and a motoneuron, it leads to a partial cell fate transformation in a specific sensory neuron class (Hobert et al., 1999). Taken together, individual *C. elegans* Lhx genes appear to have a highly context-dependent impact on neuronal differentiation.

We postulate that it is the information content of specific transcription factor codes that determines whether the loss of a Lhx gene in a given cellular context causes either a failure to differentiate or a switch to another neuronal cell fate. For example, in regard to *lim-4* function in AWB it could be envisioned that the expression of the transcription factors *a-e* defines an '*abcde*' code required for AWB development (with '*e*' being *lim-4)*, while the combination '*abcd*' defines AWC fate. Loss of *lim-4* hence leads to a switch in cell fate and the adoption of AWC fate. In the case of *ttx-3*, the transcription factor code '*fghjk*' defines AIY fate ('*k*' being *ttx-3*); however, the combination '*fghj*' has no specific coding potential and hence loss of *ttx-3* simply leads to a failure to differentiate. Note that on first sight, our proposed classification of *ttx-3* as a central regulator of AIY fate may argue that only a one letter code, '*k*', may specify AIY fate; however, our demonstration of a strict context-dependency of *ttx-3* function illustrates the need to postulate a multi-letter code. Thus, the outcome of a loss of a transcription factor in a given cell may be entirely predicted by the information content of the remainder of the transcription factor code.

A defined transcription factor code present in a postmitotic neuron at the stage of terminal differentiation may not however be the only determinant of the differentiation program of the cell; instead, in addition to the one-dimensional, spatial code of transcription factors present in a postmitotic neuron, there is also a second, temporal dimension to the differentiation program of a cell. That is, a neuron may have been exposed in its developmental history to certain determinants that have a perduring effect on the cell. Thus, an equivalent transcription factor code present in two postmitotic neurons that undergo terminal differentiation may be interpreted differentially in each cell, based on the individual history of the cell. Once the complete temporal and spatial profiles of transcription factor expression in any given neuron and its precursors is known, an achievement not too far away in a simple organism such as *C. elegans*, it may be possible to compute and model cell fates in a directed fashion.

Besides the many researchers who provided us with published strains and reporter gene reagents, we are very grateful to several people for their sharing of unpublished reagents: Tim Niacaris and Leon Avery for *ser-2::gfp*; Takeshi Ishihara and Isao Katsura for *C36B7.7::GFP*; Janet Duerr and Jim Rand for anti-UNC-17 antibodies and advice on the staining protocol; Hannes Buelow for the *otIs33* strain; Oscar Aurelio for *zig-2* and *zig-3::gfp*; Mike Nonet and Jim Rand for alleles of synaptic transmission mutants; and Ikue Mori and Hiroyuki Sasakura for providing the *nj14* allele. We thank Shawn Lockery, Piali Sengupta and Joe Culotti for providing integrants of the *gcy-5::gfp, gcy-8::gfp* and *F25B3.3::gfp* transgenes. We are grateful to Nehal Mehta for her involvement in the screens leading to the isolation of *ot22* and *ot23*; Jun Zhu and Lewis Diamond for technical assistance; Enyuan Shang for cloning the *unc-119::ttx-3* construct; and Gary Ruvkun, in whose laboratory O. H. constructed *mgIs18* and isolated the *mg158* allele. We thank Iva Greenwald for help and advice with the *lin-12* experiments; and Iva Greenwald, Gary Ruvkun, Piali Sengupta, Barth Grant, Sophie Jarriault-Reina, Richard Mann, Tom Jessell, Cori Bargmann, anonymous reviewers and members of the Hobert laboratory for comments on the manuscript. This work was funded in part by a HFSPO Research Grant to O. H., by a Culpeper Biomedical Pilot Initiative Grant and by a Herbert Irving Cancer Center Pilot Grant. O. H. is a Searle Scholar, Sloan Research Fellow and Klingenstein Fellow. Several strains were provided by the *C. elegans* Genetics Center, which is funded by the NIH.

REFERENCES

Alfonso, A., Grundahl, K., Duerr, J. S., Han, H. P. and Rand, J. B. (1993). The Caenorhabditis elegans unc-17 gene: a putative vesicular acetylcholine transporter. *Science* **261**, 617-619.

Anderson, D. J. and Jan, Y. N. (1997). The determination of the neuronal phenotype. In *Molecular and Cellular Approaches to Neural Development* (ed. M. W. Cowan, T. M. Jessell and S. L. Zipursky), pp. 26-63. Oxford: Oxford University Press.

Antebi, A., Norris, C., Hedgecock, E. M. and Garriga, G. (1997). Cell and growth cone migrations. In *C.elegans II*, (ed. D. L. Riddle, T. Blumenthal, B. J. Meyer and J. R. Priess), pp. 583-610. Cold Spring Harbor: Cold Spring Harbor Laboratory Press.

Bang, A. G. and Goulding, M. D. (1996). Regulation of vertebrate neural cell fate by transcription factors. *Curr. Opin. Neurobiol.* **6**, 25-32.

Baum, P. D. and Garriga, G. (1997). Neuronal migrations and axon fasciculation are disrupted in ina-1 integrin mutants. *Neuron* **19**, 51-62.

Baum, P. D., Guenther, C., Frank, C. A., Pham, B. V. and Garriga, G. (1999). The Caenorhabditis elegans gene ham-2 links Hox patterning to migration of the HSN motor neuron. *Genes Dev.* **13**, 472-483.

Benveniste, R. J., Thor, S., Thomas, J. B. and Taghert, P. H. (1998). Cell type-specific regulation of the Drosophila FMRF-NH2 neuropeptide gene by Apterous, a LIM homeodomain transcription factor. *Development* **125**, 4757-4765.

Cassata, G., Kagoshima, H., Andachi, Y., Kohara, Y., Durrenberger, M. B., Hall, D. H. and Burglin, T. R. (2000). The LIM homeobox gene ceh-14 confers thermosensory function to the AFD neurons in Caenorhabditis elegans. *Neuron* **25**, 587-597.

Chalfie, M. and Sulston, J. (1981). Developmental genetics of the mechanosensory neurons of Caenorhabditis elegans. *Dev. Biol.* **82**, 358-370.

Chen, C. M. and Cepko, C. L. (2000). Expression of Chx10 and Chx10-1 in the developing chicken retina. *Mech. Dev.* **90**, 293-297.

Chisholm, A. D. and Horvitz, H. R. (1995). Patterning of the Caenorhabditis elegans head region by the Pax-6 family member vab-3. *Nature* **377**, 52-55.

Colbert, H. A., Smith, T. L. and Bargmann, C. I. (1997). OSM-9, a novel protein with structural similarity to channels, is required for olfaction, mechanosensation, and olfactory adaptation in Caenorhabditis elegans. *J. Neurosci.* **17**, 8259-8269.

Culotti, J. G. (1994). Axon guidance mechanisms in Caenorhabditis elegans. *Curr. Opin. Genet. Dev.* **4**, 587-595.

Duggan, A., Ma, C. and Chalfie, M. (1998). Regulation of touch receptor differentiation by the Caenorhabditis elegans mec-3 and unc-86 genes. *Development* **125**, 4107-4119.

Ebinu, J. O., Bottorff, D. A., Chan, E. Y., Stang, S. L., Dunn, R. J. and Stone, J. C. (1998). RasGRP, a Ras guanyl nucleotide- releasing protein with calcium- and diacylglycerol-binding motifs. *Science* **280**, 1082-1086.

Edlund, T. and Jessell, T. M. (1999). Progression from extrinsic to intrinsic signaling in cell fate specification: a view from the nervous system. *Cell* **96**, 211-224.

Fitzgerald, K., Wilkinson, H. A. and Greenwald, I. (1993). glp-1 can substitute for lin-12 in specifying cell fate decisions in Caenorhabditis elegans. *Development* **119**, 1019-1027.

Forrester, W. C. and Garriga, G. (1997). Genes necessary for C. elegans cell and growth cone migrations. *Development* **124**, 1831-1843.

Forrester, W. C., Perens, E., Zallen, J. A. and Garriga, G. (1998). Identification of Caenorhabditis elegans genes required for neuronal differentiation and migration. *Genetics* **148**, 151-165.

Freyd, G., Kim, S. K. and Horvitz, H. R. (1990). Novel cysteine-rich motif and homeodomain in the product of the Caenorhabditis elegans cell lineage gene lin-11. *Nature* **344**, 876-879.

Gehring, W. J., Affolter, M. and Burglin, T. (1994). Homeodomain proteins. *Annu. Rev. Biochem.* **63**, 487-526.

George, S. E., Simokat, K., Hardin, J. and Chisholm, A. D. (1998). The VAB-1 Eph receptor tyrosine kinase functions in neural and epithelial morphogenesis in C. elegans. *Cell* **92**, 633-643.

Giniger, E., Jan, L. Y. and Jan, Y. N. (1993). Specifying the path of the intersegmental nerve of the Drosophila embryo: a role for Delta and Notch. *Development* **117**, 431-440.

Greenwald, I. S., Sternberg, P. W. and Horvitz, H. R. (1983). The lin-12 locus specifies cell fates in Caenorhabditis elegans. *Cell* **34**, 435-444.

Hallam, S., Singer, E., Waring, D. and Jin, Y. (2000). The C. elegans NeuroD homolog cnd-1 functions in multiple aspects of motor neuron fate specification. *Development* **127**, 4239-4252.

Hawkins, N. C. and McGhee, J. D. (1990). Homeobox containing genes in the nematode Caenorhabditis elegans. *Nucleic Acids Res.* **18**, 6101-6106.

Hedgecock, E. M. and Russell, R. L. (1975). Normal and mutant thermotaxis in the nematode Caenorhabditis elegans. *Proc. Natl. Acad. Sci. USA* **72**, 4061-4065.

Hedgecock, E. M., Culotti, J. G., Thomson, J. N. and Perkins, L. A. (1985). Axonal guidance mutants of Caenorhabditis elegans identified by filling sensory neurons with fluorescein dyes. *Dev. Biol.* **111**, 158-170.

Hedgecock, E. M., Culotti, J. G. and Hall, D. H. (1990). The unc-5, unc-6, and unc-40 genes guide circumferential migrations of pioneer axons and mesodermal cells on the epidermis in C. elegans. *Neuron* **4**, 61-85.

Hobert, O., Mori, I., Yamashita, Y., Honda, H., Ohshima, Y., Liu, Y. and Ruvkun, G. (1997). Regulation of interneuron function in the C. elegans thermoregulatory pathway by the ttx-3 LIM homeobox gene. *Neuron* **19**, 345-357.

Hobert, O., D'Alberti, T., Liu, Y. and Ruvkun, G. (1998). Control of neural development and function in a thermoregulatory network by the LIM homeobox gene lin-11. *J. Neurosci.* **18**, 2084-2096.

Hobert, O., Tessmar, K. and Ruvkun, G. (1999). The Caenorhabditis elegans lim-6 LIM homeobox gene regulates neurite outgrowth and function of particular GABAergic neurons. *Development* **126**, 1547-1562.

Hobert, O. and Westphal, H. (2000). Function of LIM homeobox genes. *Trends Genet.* **16**, 75-83.

Jin, Y., Jorgensen, E., Hartwieg, E. and Horvitz, H. R. (1999). The *Caenorhabditis elegans* gene *unc-25* encodes glutamic acid decarboxylase and is required for synaptic transmission but not synaptic development. *J. Neurosci.* **19**, 539-548.

Johnstone, D. B., Wei, A., Butler, A., Salkoff, L. and Thomas, J. H. (1997). Behavioral defects in C. elegans egl-36 mutants result from potassium channels shifted in voltage-dependence of activation. *Neuron* **19**, 151-164.

Jurata, L. W., Thomas, J. B. and Pfaff, S. L. (2000). Transcriptional mechanisms in the development of motor control. *Curr Opin Neurobiol* **10**, 72-79.

Kania, A., Johnson, R. L. and Jessell, T. M. (2000). Coordinate roles for LIM homeobox genes in directing the dorsoventral trajectory of motor axons in the vertebrate limb. *Cell* **102**, 161-173.

Kawasaki, H., Springett, G. M., Toki, S., Canales, J. J., Harlan, P., Blumenstiel, J. P., Chen, E. J., Bany, I. A., Mochizuki, N., Ashbacher, A. et al. (1998). A Rap guanine nucleotide exchange factor enriched highly in the basal ganglia. *Proc. Natl. Acad. Sci. USA* **95**, 13278-13283.

Li, W., Herman, R. K. and Shaw, J. E. (1992). Analysis of the Caenorhabditis elegans axonal guidance and outgrowth gene unc-33. *Genetics* **132**, 675-689.

Lundgren, S. E., Callahan, C. A., Thor, S. and Thomas, J. B. (1995). Control of neuronal pathway selection by the Drosophila LIM homeodomain gene apterous. *Development* **121**, 1769-1773.

Maduro, M. and Pilgrim, D. (1995). Identification and cloning of unc-119, a gene expressed in the Caenorhabditis elegans nervous system. *Genetics* **141**, 977-988.

McIntire, S. L., Garriga, G., White, J., Jacobson, D. and Horvitz, H. R. (1992). Genes necessary for directed axonal elongation or fasciculation in C. elegans. *Neuron* **8**, 307-322.

Mitani, S., Du, H., Hall, D. H., Driscoll, M. and Chalfie, M. (1993). Combinatorial control of touch receptor neuron expression in Caenorhabditis elegans. *Development* **119**, 773-783.

Mori, I. and Ohshima, Y. (1995). Neural regulation of thermotaxis in Caenorhabditis elegans. *Nature* **376**, 344-348.

Nelson, L. S., Rosoff, M. L. and Li, C. (1998). Disruption of a neuropeptide gene, flp-1, causes multiple behavioral defects in Caenorhabditis elegans. *Science* **281**, 1686-1690.

Peckol, E. L., Zallen, J. A., Yarrow, J. C. and Bargmann, C. I. (1999). Sensory activity affects sensory axon development in C. elegans. *Development* **126**, 1891-1902.

Pfaff, S. L., Mendelsohn, M., Stewart, C. L., Edlund, T. and Jessell, T. M. (1996). Requirement for LIM homeobox gene Isl1 in motor neuron generation reveals a motor neuron-dependent step in interneuron differentiation. *Cell* **84**, 309-320.

Rand, J. B. and Nonet, M. L. (1997). Synaptic Transmission. In *C.elegans II*, (ed. D. L. Riddle, T. Blumenthal, B. J. Meyer and J. R. Priess), pp. 611-644. Cold Spring Harbor: Cold Spring Harbor Laboratory Press.

Richmond, J. E., Davis, W. S. and Jorgensen, E. M. (1999). UNC-13 is required for synaptic vesicle fusion in C. elegans. *Nat. Neurosci.* **2**, 959-964.

Sagasti, A., Hobert, O., Troemel, E. R., Ruvkun, G. and Bargmann, C. I. (1999). Alternative olfactory neuron fates are specified by the LIM homeobox gene lim-4. *Genes Dev.* **13**, 1794-1806.

Schackwitz, W. S., Inoue, T. and Thomas, J. H. (1996). Chemosensory neurons function in parallel to mediate a pheromone response in C. elegans. *Neuron* **17**, 719-728.

Sengupta, P., Chou, J. H. and Bargmann, C. I. (1996). odr-10 encodes a seven transmembrane domain olfactory receptor required for responses to the odorant diacetyl. *Cell* **84**, 899-909.

Sestan, N., Artavanis-Tsakonas, S. and Rakic, P. (1999). Contact-dependent inhibition of cortical neurite growth mediated by notch signaling. *Science* **286**, 741-746.

Sharma, K., Sheng, H. Z., Lettieri, K., Li, H., Karavanov, A., Potter, S., Westphal, H. and Pfaff, S. L. (1998). LIM homeodomain Factors Lhx3 and Lhx4 assign subtype identities for motor neurons. *Cell* **95**, 817-828.

Sulston, J. E. (1983). Neuronal cell lineages in the nematode Caenorhabditis elegans. *Cold Spring Harb. Symp. Quant. Biol.* **48**, 443-452.

Sulston, J. E., Schierenberg, E., White, J. G. and Thomson, J. N. (1983). The embryonic cell lineage of the nematode Caenorhabditis elegans. *Dev. Biol.* **100**, 64-119.

Svendsen, P. C. and McGhee, J. D. (1995). The C. elegans neuronally expressed homeobox gene ceh-10 is closely related to genes expressed in the vertebrate eye. *Development* **121**, 1253-1262.

Sze, J. Y., Victor, M., Loer, C., Shi, Y. and Ruvkun, G. (2000). Food and metabolic signalling defects in a Caenorhabditis elegans serotonin-synthesis mutant. *Nature* **403**, 560-564.

Tanabe, Y., William, C. and Jessell, T. M. (1998). Specification of motor neuron identity by the MNR2 homeodomain protein. *Cell* **95**, 67-80.

Thor, S. and Thomas, J. B. (1997). The Drosophila islet gene governs axon pathfinding and neurotransmitter identity. *Neuron* **18**, 397-409.

Thor, S., Andersson, S. G., Tomlinson, A. and Thomas, J. B. (1999). A LIM-homeodomain combinatorial code for motor-neuron pathway selection. *Nature* **397**, 76-80.

Troemel, E. R., Chou, J. H., Dwyer, N. D., Colbert, H. A. and Bargmann, C. I. (1995). Divergent seven transmembrane receptors are candidate chemosensory receptors in C. elegans. *Cell* **83**, 207-218.

Troemel, E. R., Kimmel, B. E. and Bargmann, C. I. (1997). Reprogramming chemotaxis responses: sensory neurons define olfactory preferences in C. elegans. *Cell* **91**, 161-169.

Tsuchida, T., Ensini, M., Morton, S. B., Baldassare, M., Edlund, T., Jessell, T. M. and Pfaff, S. L. (1994). Topographic organization of embryonic motor neurons defined by expression of LIM homeobox genes. *Cell* **79**, 957-970.

Wang, B. B., Muller-Immergluck, M. M., Austin, J., Robinson, N. T., Chisholm, A. and Kenyon, C. (1993). A homeotic gene cluster patterns the anteroposterior body axis of C. elegans. *Cell* **74**, 29-42.

Way, J. C. and Chalfie, M. (1988). mec-3, a homeobox-containing gene that specifies differentiation of the touch receptor neurons in C. elegans. *Cell* **54**, 5-16.

Weinshenker, D., Wei, A., Salkoff, L. and Thomas, J. H. (1999). Block of an ether-a-go-go-like K(+) channel by imipramine rescues egl-2 excitation defects in caenorhabditis elegans. *J. Neurosci.* **19**, 9831-9840.

White, J. G., Southgate, E., Thomson, J. N. and Brenner, S. (1986). The structure of the nervous system of the nematode *Caenorhabditis elegans. Philos. Trans. Royal Soc. London Ser. B. Biol. Sci.* **314**, 1-340.

Wittenburg, N., Eimer, S., Lakowski, B., Rohrig, S., Rudolph, C. and Baumeister, R. (2000). Presenilin is required for proper morphology and function of neurons in C. elegans. *Nature* **406**, 306-309.

Wu, G. Y. and Cline, H. T. (1998). Stabilization of dendritic arbor structure in vivo by CaMKII. *Science* **279**, 222-226.

Yu, S., Avery, L., Baude, E. and Garbers, D. L. (1997). Guanylyl cyclase expression in specific sensory neurons: a new family of chemosensory receptors. *Proc. Natl. Acad. Sci. USA* **94**, 3384-3387.

Zallen, J. A., Yi, B. A. and Bargmann, C. I. (1998). The conserved immunoglobulin superfamily member SAX-3/Robo directs multiple aspects of axon guidance in C. elegans. *Cell* **92**, 217-227.

Zallen, J. A., Kirch, S. A. and Bargmann, C. I. (1999). Genes required for axon pathfinding and extension in the C. elegans nerve ring. *Development* **126**, 3679-3692.

Zhao, C. and Emmons, S. W. (1995). A transcription factor controlling development of peripheral sense organs in C. elegans. *Nature* **373**, 74-78.

Zhao, H. and Nonet, M. L. (2000). A retrograde signal is involved in activity-dependent remodeling at a C. elegans neuromuscular junction. *Development* **127**, 1253-1266.

Zwaal, R. R., Broeks, A., van Meurs, J., Groenen, J. T. and Plasterk, R. H. (1993). Target-selected gene inactivation in Caenorhabditis elegans by using a frozen transposon insertion mutant bank. *Proc. Natl. Acad. Sci. USA* **90**, 7431-7435.